N73-14891

ANNUAL REPORT

FOR

EXPLOSIVE SHOCK DAMAGE POTENTIAL

IN SPACE STRUCTURES

drexel university

DREXEL UNIVERSITY
SCIENCE INDUSTRY ART
1891

DREXEL UNIVERSITY

WAVE PROPAGATION RESEARCH CENTER

PHILADELPHIA, PENNSYLVANIA

September 29, 1972

ANNUAL REPORT

FOR

EXPLOSIVE SHOCK DAMAGE POTENTIAL

IN SPACE STRUCTURES

Richard W. Mortimer

July 1, 1971 to September 30, 1972

NASA Grant NGR 39-004-041

Structures Division

Langley Research Center

TABLE OF CONTENTS

ABSTRACT

This Report contains the results of a one year study into the effects of a pulse shape on the transient response of a cylindrical shell. Uniaxial, membrane, and bending theories for isotropic shells were used in this study. In addition to the results of the above analytical study, the preliminary results of an experimental study into the generation and measurement of shear waves in a cylindrical shell are included.

NOMENCLATURE

K^2 = shear correction factor

c_p^2 = plate velocity = $\frac{E}{\rho(1-\nu^2)}$

c_s^2 = shear velocity = $K \frac{G}{\rho}$

t_o = pulse duration

$\bar{\tau}$ = dimensionless time = $\frac{t\, C_p}{h}$

$\bar{\tau}_o$ = dimensionless pulse duration

λ = equivalent pulse length = $C_p t_o$

$\bar{\lambda}$ = dimensionless pulse length = $\bar{\tau}_o$

Other symbols are defined in text

I. INTRODUCTION

Included in this Report are the results of a one year study performed for the Structures Division of NASA - Langley Research Center. The major tasks of this study were:

1. An analytical parametric study to determine the effect of pulse shape (e.g. magnitude, shape, duration, rise time) on the transient response of cylindrical shells subjected to longitudinal impacts,
2. An analytical parametric study to determine the effect of pulse shape on the transient response of cylindrical shells having geometrical discontinuities (e.g. discontinuity in thickness) subjected to longitudinal impacts,
3. An evaluation of the importance of secondary shell theory terms (e.g. transverse shear deformation, radial and rotary inertia, and bending) in predicting transient responses of cylindrical shells subjected to axial impacts.

In addition to the above tasks, an experimental program was initiated to develop a technique for generating shear waves in a cylindrical shell. The initial results of this program, including the measured shear wave velocities, are also included in this Report.

II. SOLUTION OF THE MEMBRANE SHELL EQUATIONS BY THE METHOD OF CHARACTERISTICS

Since part of our task in this grant was to determine the effect of the higher order shell terms (eg rotary inertia, transverse shear strain, bending) on the predicted responses of cylindrical shells subjected to longitudinal impact, we decided to attempt the solution of the classical membrane equations by the method of characteristics. The first point to be mentioned is that the classical membrane equations do not constitute a system of completely hyperbolic partial differential equations. The method of characteristics is only applicable to hyperbolic systems of equations. Obviously the application of the method of characteristics to a non-hyperbolic system of equations is suspected. Before discussing the numerical approach used here to achieve this apparent misapplication of a mathematical technique, we shall describe the classical membrane equations.

The equations of motion of a cylindrical membrane under axisymmetric conditions are (see Appendix A for equations of all shell theories used)

$$\frac{\partial N_x}{\partial x} = h\rho \frac{\partial^2 u}{\partial t^2}$$

$$-\frac{N_\theta}{R} = h\rho \frac{\partial^2 w}{\partial t^2} \qquad \text{(II-1)}$$

and the strain-displacement and stress-strain relations are

$$\varepsilon_{xx} = \frac{\partial u}{\partial x} \quad , \quad \varepsilon_{\theta\theta} = \frac{w}{R} \qquad \text{(II-2)}$$

$$N_x = \frac{Eh}{1-\nu^2} \left[\varepsilon_{xx} + \nu\, \varepsilon_{\theta\theta} \right] \; ; \; N = \frac{Eh}{1-\nu^2} \left[\varepsilon_{\theta\theta} + \nu\, \varepsilon_{xx} \right]$$

where N_x, ε_{xx}, and u are the stress, strain, and displacement in the axial direction; N_θ and $\varepsilon_{\theta\theta}$ the stress and strain in the circumferential directions; w the displacement in radial direction; h and R the shell thickness and radius.

Substituting equations (II-2) into (II-1) yields the classical membrane equations in terms of the two displacements. These are

$$\frac{\partial^2 u}{\partial x^2} - \frac{1}{c_p^2}\frac{\partial^2 u}{\partial t^2} = -\frac{\nu}{R}\frac{\partial w}{\partial x}$$

$$-\rho\frac{\partial^2 w}{\partial t^2} = \frac{E}{1-\nu^2}\left[\frac{w}{R} + \nu\frac{\partial u}{\partial x}\right] \tag{II-3}$$

where $c_p^2 = E/\rho(1-\nu^2)$ called the plate velocity. As we see, this system of equations is not completely hyperbolic. The first equation can be considered to be hyperbolic (the left-hand side is of the form of the simple wave equation) while the second equation is parabolic in nature. In order to understand our reasoning, soon to be introduced, let me describe another "membrane" theory which will incorporate the effect of the transverse shear force into the classical membrane formulation. For this case the "membrane" equation of motion are (Ref. 1)

$$\frac{\partial N_x}{\partial x} = \rho h\frac{\partial^2 u}{\partial t^2}$$

$$\frac{\partial Q_x}{\partial x} - \frac{N_\theta}{R} = \rho h\frac{\partial^2 w}{\partial t^2} \tag{II-4}$$

where in addition to the relation of (II-2) we now have

$$\gamma_{xz} = \frac{\partial w}{\partial x} \text{ and } Q_x = K^2\gamma_{xz} = K^2 G\frac{\partial w}{\partial x} \tag{II-5}$$

where G is the shear modulus, Q_x the transverse shear stress, γ_{xz} the transverse shear strain, and K^2 the shear correction factor. Substitution of equations (II-2) and (II-5) into (II-4) yields the system of equations

$$\frac{\partial^2 u}{\partial x^2} - \frac{1}{c_p^2}\frac{\partial^2 u}{\partial t^2} = -\frac{\nu}{R}\frac{\partial w}{\partial x}$$

$$\frac{\partial^2 w}{\partial x^2} - \frac{1}{c_s^2}\frac{\partial^2 w}{\partial t^2} = \frac{1}{\rho c_s^2}\frac{E}{(1-\nu^2)}\left(\frac{w}{R} + \nu\frac{\partial u}{\partial x}\right) \qquad \text{(II-6)}$$

where $c_s^2 = K^2G/\rho$ is called the shear velocity. Equation (II-6) is a completely hyperbolic system of partial differential equations; disturbances in u will propagate with the plate velocity, c_p, and disturbances in w will propagate with the shear velocity, c_s. We can now see, conceptually, the difference in physical interpretation between equations (II-3) and (II-6). If in the second of equations (I-6) we multiply through by c_s^2 (or K^2) and then let c_s^2 go to zero we see that eq. (II-6) reduces to eq. (II-3). So, our numerical procedure used here will be to solve eq. (II-6), but, we will require c_s^2 to be extremely small, <u>but</u>, not zero. In other words, we will actually be solving the systems of equations (II-6), but, due to the smallness of c_s^2 we are physically approximating equations (II-3). The question now arises, the application of the method of characteristics to equations (II-3) has been a standard technique so why this procedure? The answer is simply this. When people do apply the method of characteristics to equations (II-3) in order to analyze a cylindrical shell impact problem they <u>always consider a semi-infinite medium</u>. The reason for this is simple, this standard technique does not permit the incorporation of a boundary condition in w (remember a term $\frac{\partial w}{\partial x}$ appears in the governing equations). So, at the impacted end a boundary condition in u is prescribed and the other end is assumed to be at infinity, thus, the question of imposing one boundary condition in w is avoided. With our procedure outlined here we are able to mathematically incorporate all the boundary conditions properly. The only point to be demonstrated is whether our solution of equations (II-6) with c_s (K) very small yields, for practical purposes, the solution to the classical membrane equations.

We ran some test cases to numerically determine how small c_s^2 must be. Our procedure was to use MCDIT-21 (Ref. 2) to solve equations (II-6) subjected to impact boundary conditions at x=0, or,

$$\frac{\partial u}{\partial t}(0,t) = V$$

$$G\,K^2 \frac{\partial w}{\partial x}(0,t) = 0$$

We used the shear correction factor, K^2, as our parameter to vary the shear velocity, c_s (remember $c_s^2 = K^2 G/\rho$); the value of K^2 is approximately 0.87 for most shell problems involving shear waves. We calculated the transient responses of a typical cylindrical shell subjected to axial impacts with different values of K^2. We then compared the strains at a particular point as predicted by each run. When the strain predictions did not significantly change with a further reduction in K^2 we chose that value of K^2 for our later studies involving the classical membrane theory. As an indication of our K^2 study, Table (II -1) shows the comparison of longitudinal strain at a distance 60 thicknesses from the impacted end for various values of K^2.

TABLE (II -1)

K^2	$\varepsilon_{xx}(x=60)/\varepsilon_{xx}(x=0)$
0.87	.75649
0.87×10^{-4}	.77251
0.87×10^{-6}	.77318
0.87×10^{-8}	.77391
0.87×10^{-10} (double precision)	.77225

We can see from Table (II -1) that, numerically, once K^2 has reached the value of 0.87×10^{-4} there is no significant change in the strain predictions with a further reduction in K^2. Except for the last entry all other calculations were performed in single precision.

In order to determine the exactness of our technique for solving the classical membrane equations we compared our solution to the Laplace transform solution of the classical membrane equations as published by Berkowitz (Ref. 3). In his paper, the author analyzes the response of a semi-infinite elastic cylindrical shell subjected to a longitudinal impact. He solves a system of equations identical to (II -3), subjected to impact conditions at $\bar{x}=0$, by applying asymptotic expansion techniques to the Laplace transform inversion integrals. He calculates the longitudinal stress at a dimensionless time as it varies with dimensionless axial distance. Figure 1 shows his results as compared to our results for $K^2 = 0.87 \times 10^{-8}$. The fact that our results (for $K^2 = 0.87 \times 10^{-8}$) and his do not agree identically is to be expected since both are approximate solutions to the same governing equations.

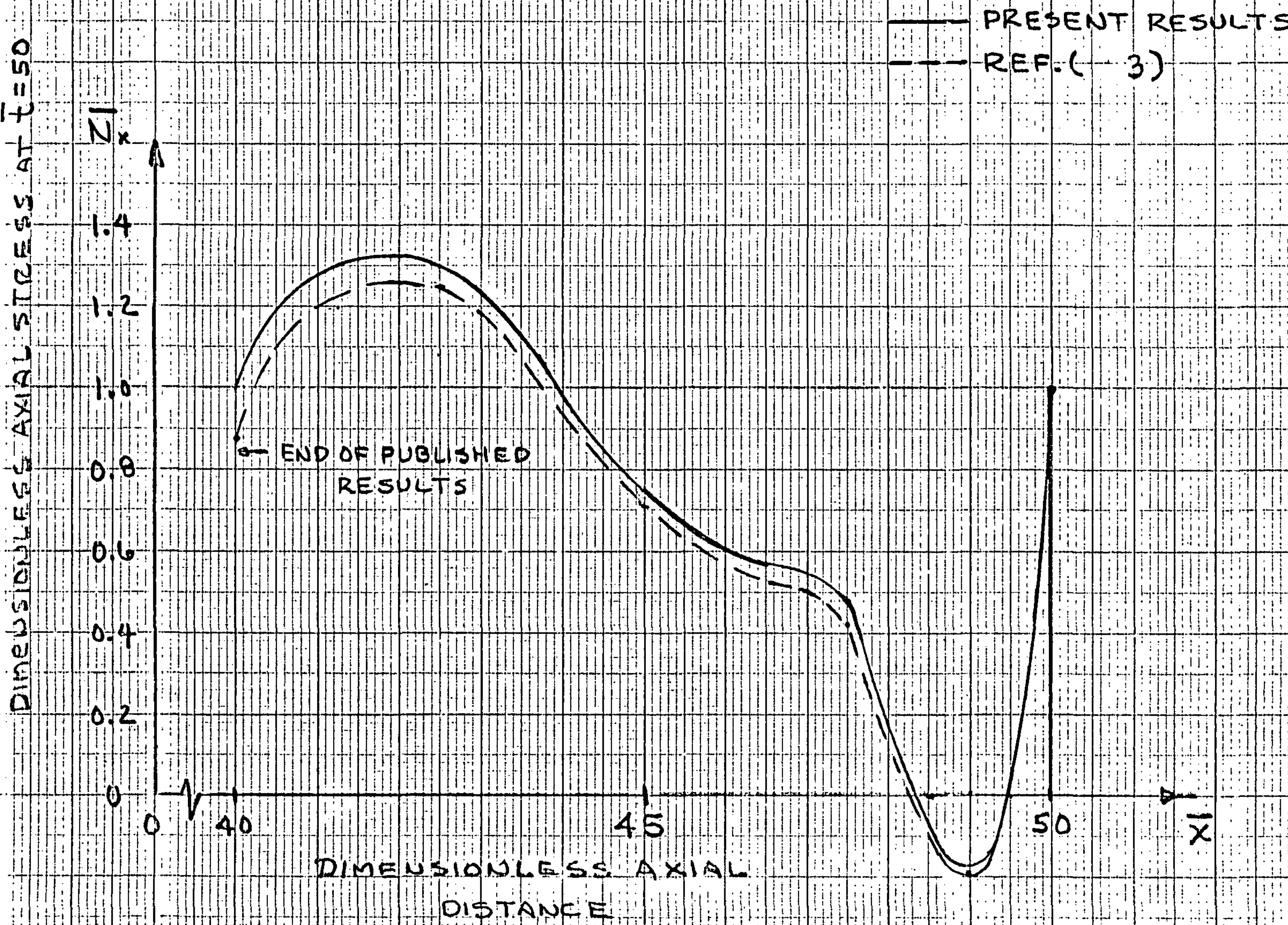

FIGURE 1 COMPARISON OF MEMBRANE SOLUTIONS AT $\bar{t}=50$.

III. PULSE SYNTHESIS FOR DETERMINING TRANSIENT RESPONSE OF SHELL DUE TO PULSES OF DIFFERENT SHAPES

A major portion of this research project was to determine the effect of pulse shape (e.g. rise time, pulse duration, shape) on the transient response of cylindrical shells subjected to longitudinal impact loading. One approach for achieving this phase of the research is to utilize our computer codes (MCDIT-21 and MCDU-26) and make numerous runs where we vary the shapes, rise times, and pulse durations. The result of this type of approach would be numerous parametric plots. Another approach would be to determine a set of "building blocks" which could be used to approximate the different pulse shapes and then we need only evaluate and understand the response of the shell to these "building block" functions. Once we understand this then we need only superimpose the resulting responses linearly and we can understand the response to the original pulse shapes of interest. This letter concept is not new; people have discussed the use of rectangular functions as "building blocks" for such a purpose. However, we discarded this type of function for our analysis due to the large number which would be needed to describe the pulse shape functions used in our study. The approach we finally chose to achieve this phase of our research was a combination of both. In otherwords, we performed some computer runs with the exact shapes in order to isolate important parameters of the pulse and then we used the second approach to try and understand these initial results and predict responses with further variations of the parameter. In this Section of the Report we will discuss the pulse shapes used in our study, the "building block" approach, and the response of the cylindrical shell to these "building block" pulses. In the next Section of the Report, we will discuss the exact approach, the use of the "building blocks", and the results of our pulse shape study.

III. 1 Pulse Shapes

We decided to limit the number of pulse shapes to those shown in Figure 2. The reason we chose these shapes is that we felt that each shape or combination of shapes was of practical interest. For example, if we understood the response of the shell to shape 2a and 2b we could then understand the response to a pulse whose rise time ranged from 0 to $\bar{\tau}_0/2$ (see Figure 3a). This latter shape can be seen to closely represent a typical explosive pulse (Figure 3b). Other practical pulse shapes can be seen to be composed of the shapes shown in Figure 2. One last point should be made here. Each of the shapes shown in Figure 2 yield identical impulse values so that when we compared the responses due to these shapes there was no difference in energy input.

III. 2 "Building Block" Synthesis

The essence of this principle, for linear differential equations, is simply as follows:

if

$$a(\text{Input A}) + b(\text{Input B}) \approx (\text{Input C})$$

then

$$a(\text{Solution for A}) + b(\text{Solution for B}) \approx \text{Solution for C}$$

where a and b are linear coefficients. In otherwords, if we can represent a particular function by a linear combination of approximating functions then we can approximate the solution for the original function by superimposing the solutions for the approximating functions.

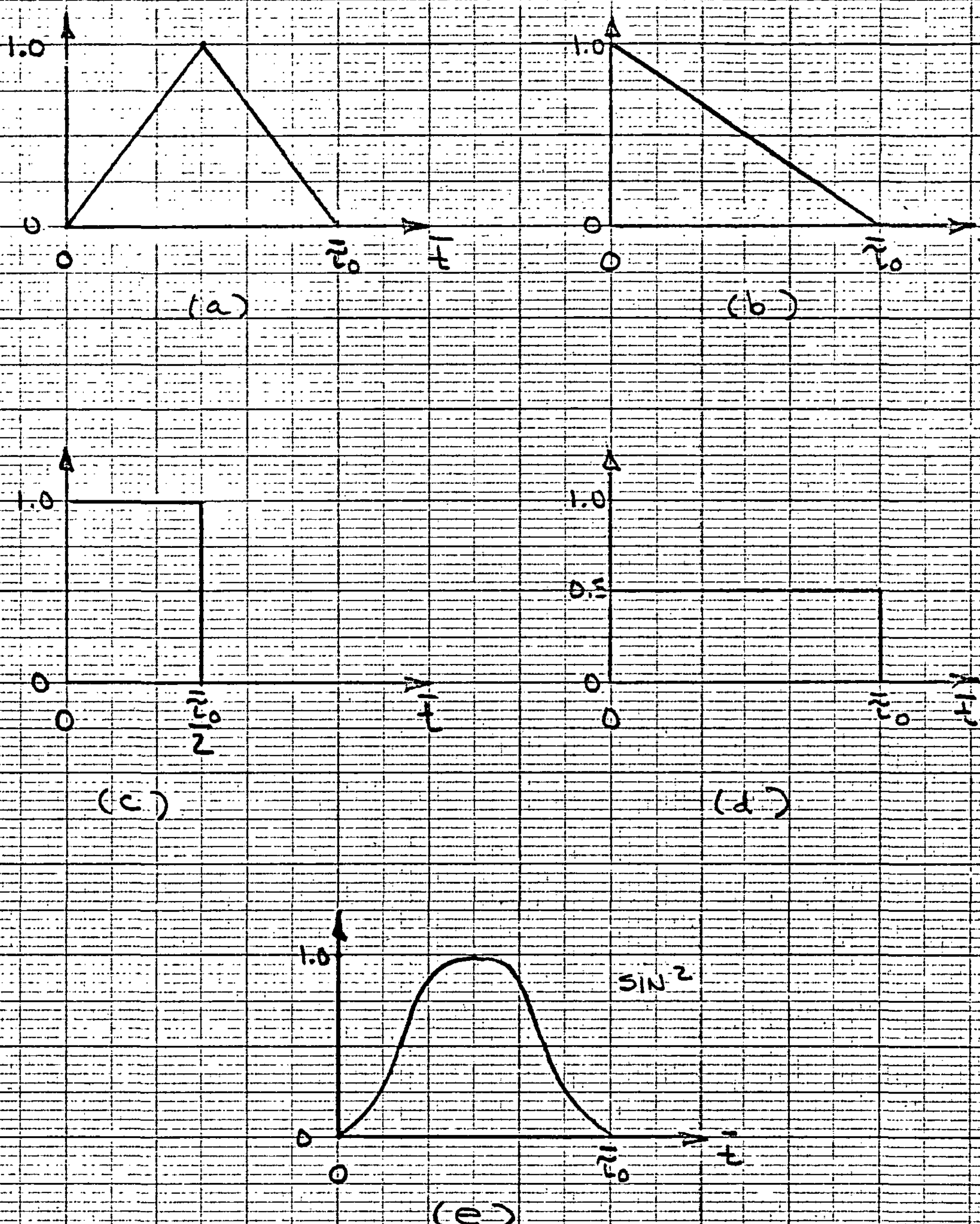

NOTE: FOR A GIVEN PULSE DURATION, $\bar{\tau}_0$, ALL THE ABOVE SHAPES YIELD IDENTICAL IMPULSE, $\bar{\tau}_0/2$.

FIGURE 2 - PULSE SHAPES USED IN BOUNDARY CONDITIONS

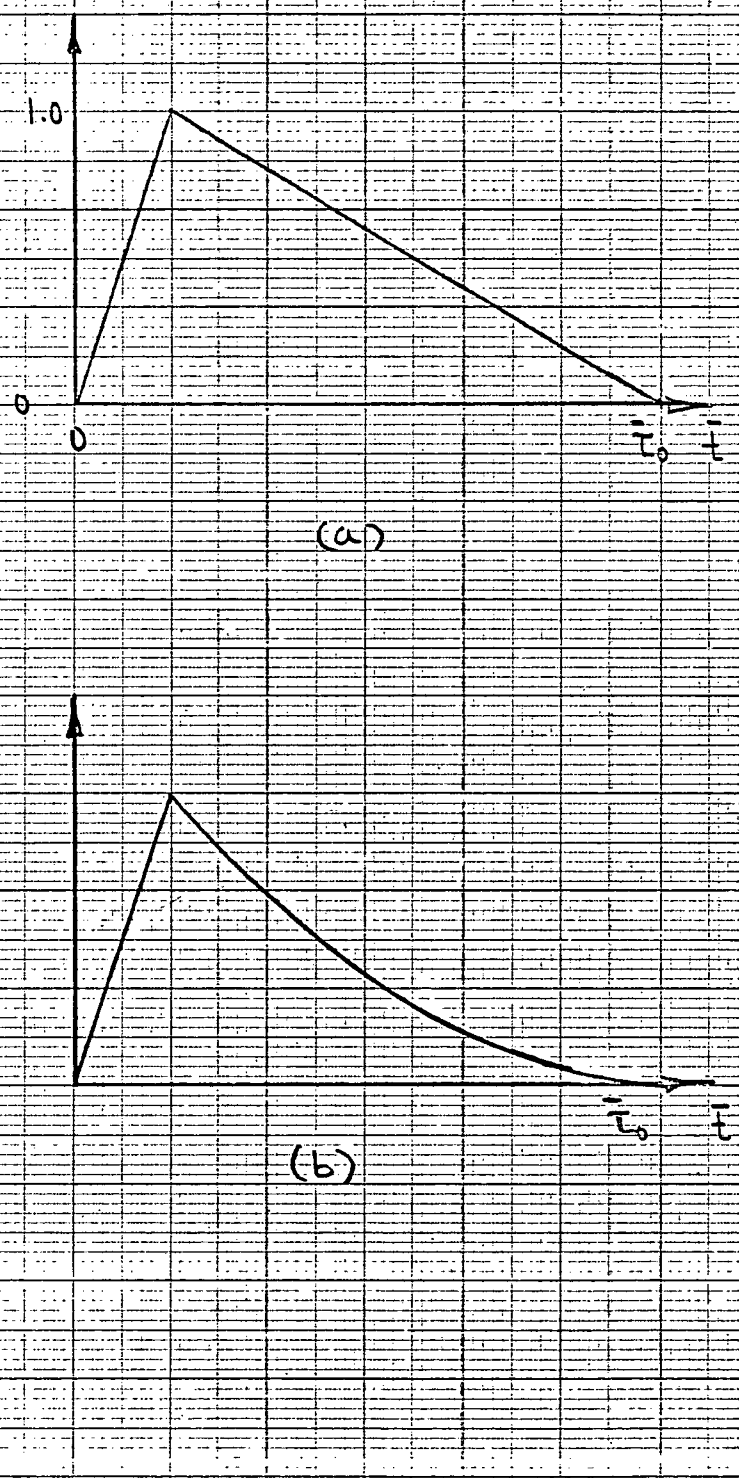

FIGURE 3 - ARBITRARY SHAPES

Before describing in detail our search for these approximating functions ("building blocks") we should define a few terms used in the discussion

Zero order discontinuity - discontinuity in magnitude only

First order discontinuity - discontinuity in first derivative only

Nth order discontinuity - discontinuity in Nth order derivative only

Approximate linear relation is

$$F(t) = A_1 V_1(t) + A_2 V_2(t) + A_3 V_3(t) \ldots.$$

where

$F(t)$ - approximated function

$V_1(t)$, $V_2(t)$, $V_3(t)$ - approximating functions

A_1, A_2, A_3 - linear coefficients

In our search for the approximating functions we had two obvious requirements. First, these functions must be able to approximate the five shapes of interest (Figure 2) and, second, the deviation between the exact shapes and the combination of these approximating functions should be small with only a few number of these functions being used. Once the approximating functions were determined we used a least squares technique to determine the linear coefficients A_1, A_2, etc. A computer program was written to facilitate the determination of these coefficients for any shape approximation. In addition, this program plotted the approximated shape based on the number of approximating functions desired. This computer program is contained in Appendix B.

Described below are some of the approximating functions considered

A. Fourier Series - Single Pulse

The initial specifications for the approximating functions was that they should have no zero order discontinuity at the origin and they should be continuous from 0+ to + ∞ (should not have a discontinuity of any order in the 0+ to + ∞ region). The above requirements are immediately satisfied by the sine series. ($\sin n\pi t$; $n = 1,2,3 \ldots$) The cosine series was not considered because of the zero order discontinuity on the origin. Due to the nature of the approximation and due to the fact that the sine series is periodic, one single pulse can not be approximated. For example; when the square pulse is approximated what in effect has been created is a new periodic function consisting of a series of square pulses.

B. Fourier Series - Compound Pulse

Observing the results of the previous example we see that an approximation of a pulse by a continuous periodic series produces another series. To partly alleviate the above problem at new pulse is created, which is composed of the original pulse plus a finite zero region. The Fourier series approximation produces again a new series, but it is hoped in this case, if the zero region length is quite large with respect to the square pulse length, and the approximation is reasonable, for all practical purposes it will mathematically satisfy the requirements of a pulse.

This compound pulse however can not be easily approximated. The results shown in Figure 4 indicate that even after ten terms the approximation was still quite poor.

C. Fourier Integral

The pulses can be approximated by continuous periodic functions not by a series, but rather by a continuous integral. This is of course useless for the study because no discrete functions can be extracted.

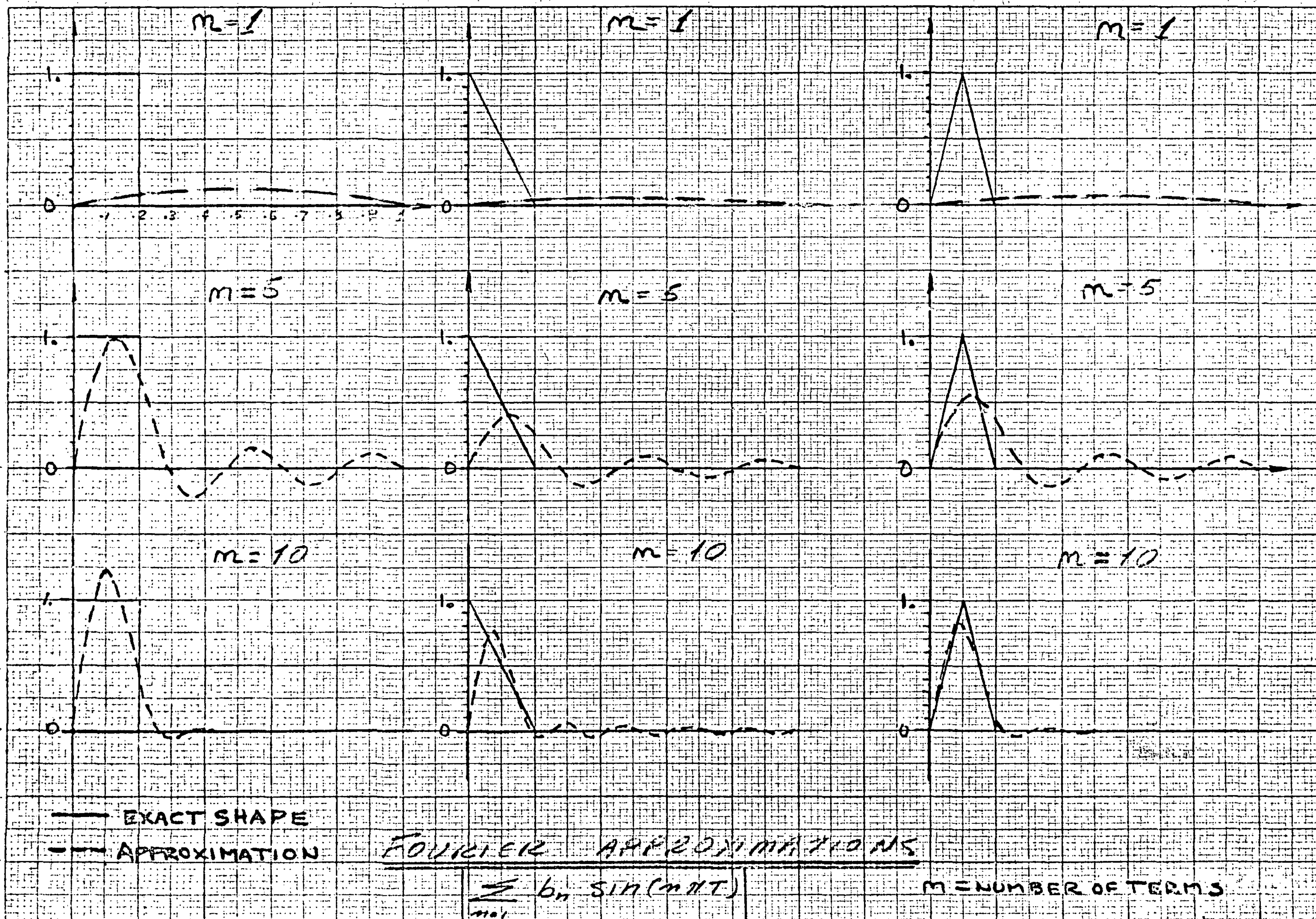

FIGURE 4 - REPRESENTATION OF PULSE SHAPES BY FOURIER - COMPOUND PULSE

D. The Envelope Function

Certain continuous functions can form a pulse of a variety of shapes as was shown by the Fourier integral. The Fourier integral though is difficult to evaluate. Another function that forms a square pulse is

e^{-t^m} As "m" approaches + ∞ function becomes square

This envelope function can be used as a multiplier for other Fourier series. The use of the envelope is to accentuate the part of the periodic series which represents the pulse.

E. Raising Sine to a Power

For the sake of interest the sine series was raised to a reciprocal power and its approximating ability was observed. This widening effect was excellent for approximating the square pulse but it failed on the triangular pulses.

F. Creating a Function

In our study we are limited to only the use of three approximating functions. This means that the approximations will be poor especially for the type of functions of interest. To alleviate this problem a special set of approximating functions are created. These functions can be made to form an almost exact fit to the pulses under consideration. One effective way of accomplishing this is by replacing some sine functions by polynomials.

G. Removing Unwanted Portion of Fourier Functions

From part "A" we see that the Fourier series produces periodic functions instead of pulses. Instead of using the complete function, we will only utilize the portion up to $\bar{\tau}_0$. For the sine series however, by removing the unwanted portion of the periodic function you introduce discontinuities of order one and higher. The utilization of this technique to represent our pulse shapes is demonstrated in Figures 5 (three terms) and 6 (five terms).

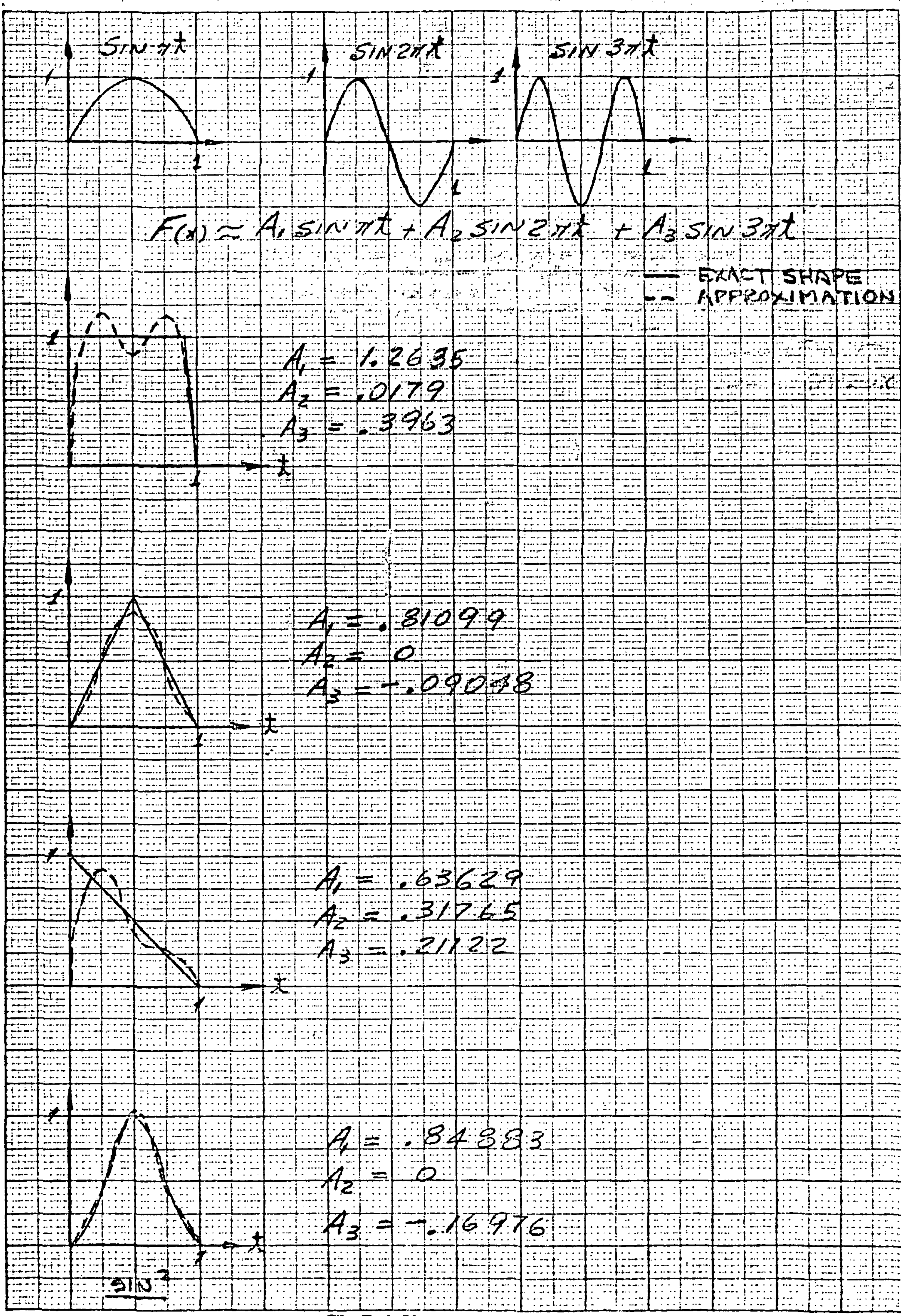

FIGURE 5 - THREE TERM APPROXIMATION

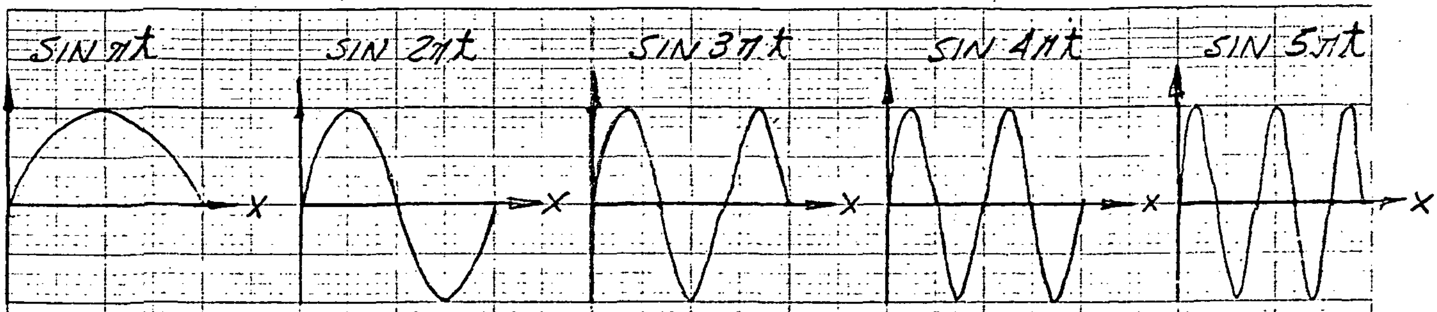

$$F(x) \simeq A_1 \sin \pi t + A_2 \sin 2\pi t + A_3 \sin 3\pi t + A_4 \sin 4\pi t + A_5 \sin 5\pi t$$

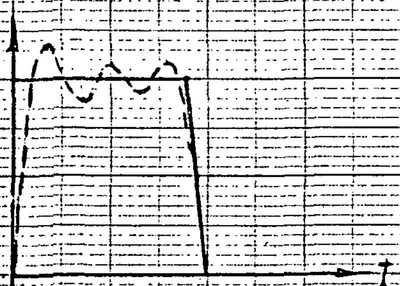

$A_1 = 1.2635$
$A_2 = 0.0179$
$A_3 = 0.3963$
$A_4 = 0.0338$
$A_5 = 0.2108$

——— EXACT SHAPE
- - - APPROXIMATION

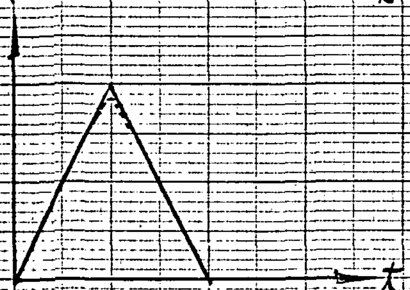

$A_1 = .81098$
$A_2 = 0$
$A_3 = -0.09048$
$A_4 = 0$
$A_5 = 0.03284$

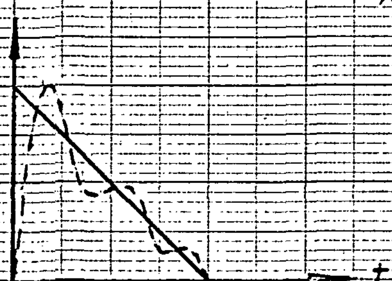

$A_1 = -.63629$
$A_2 = -.31765$
$A_3 = -.21122$
$A_4 = .15784$
$A_5 = .12568$

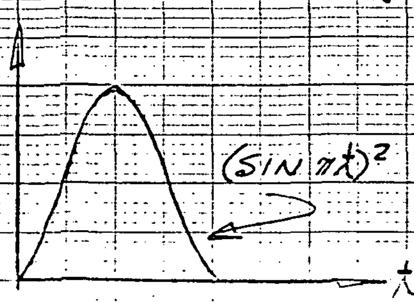

$A_1 = .84883$
$A_2 = 0$
$A_3 = -.169764$
$A_4 = 0$
$A_5 = -.024250$

FIGURE 6 – FIVE TERM APPROXIMATIONS

SUMMARY

1. A continuous set of sine functions cannot be used since the approximation creates another periodic function instead of a single pulse.
2. A Fourier integral cannot be used since it is not composed of a sum of discrete functions.
3. The envelope can be used but it is necessary since first order discontinuities are not harmful for computer applications.
4. Raising a sine to a power increases the deviation for some of the shapes.
5. Replacing some of the sine functions by polynomials is only useful for obtaining accurate approximations to only a limited number of pulses.
6. Using the sine series and removing the portion of the functions after $\bar{\tau}_0$ can be used. The only problem here is due to the first and higher order discontinuities which are introduced by removing part of the function. For computer applications, however, this problem is negligible.

Having decided on the last approximation technique we decided to compare the results of a three term approximation for a rectangular pulse with the results obtained for the exact shape. The problem we chose was that of the longitudinal impact of a cylindrical aluminum shell ($h/R = 0.049$). The boundary conditions for this problem were $M_x = Q_x = 0$ and

$$\dot{u}(0, t) = 75 \text{ in/sec} \quad ; \quad 0 \le t \le 21 \ \mu\text{sec}$$

$$N_x(0,t) = 0 \quad ; \quad 21 \ \mu\text{sec} < t$$

In otherwords, the pulse shape was rectangular. We used the three term approximation for the rectangular pulse (see Figure 5). We then solved the governing system of equations, eq. A-1, for the bending theory (k^2 - .87) for each of the three approximating sine functions. The longitudinal strain, ε_x, at X=0 and 3 inches for each of these functions is shown separately in Figures 7a and b. We then superimposed the response of each function (by use of the linear coefficients of Figure 5) and compared the resulting response with those of the numerical solution using the exact shape and experimental results. The longitudinal and circumferential strain comparisons are shown in Figures 8a and b. We see that the three terms approximation solution agrees quite well with the solution* for the exact shape.

III. 3 Transient Response of the Sine Approximating Functions

Our next step in the "building block" approach was to evaluate the transient response of a cylindrical shell to the sine pulse, the function chosen as our approximating function. Of course, by following this approach of determining the effect of pulse shape on a shell's response we eliminate a parameter, namely, the actual shape of the pulse (including rise time). Our remaining parameter is the

*Both of the solutions were based on the bending theory, eq. A-1.

FIGURE 7 RESPONSE OF CYLINDRICAL SHELL TO SINE PULSES

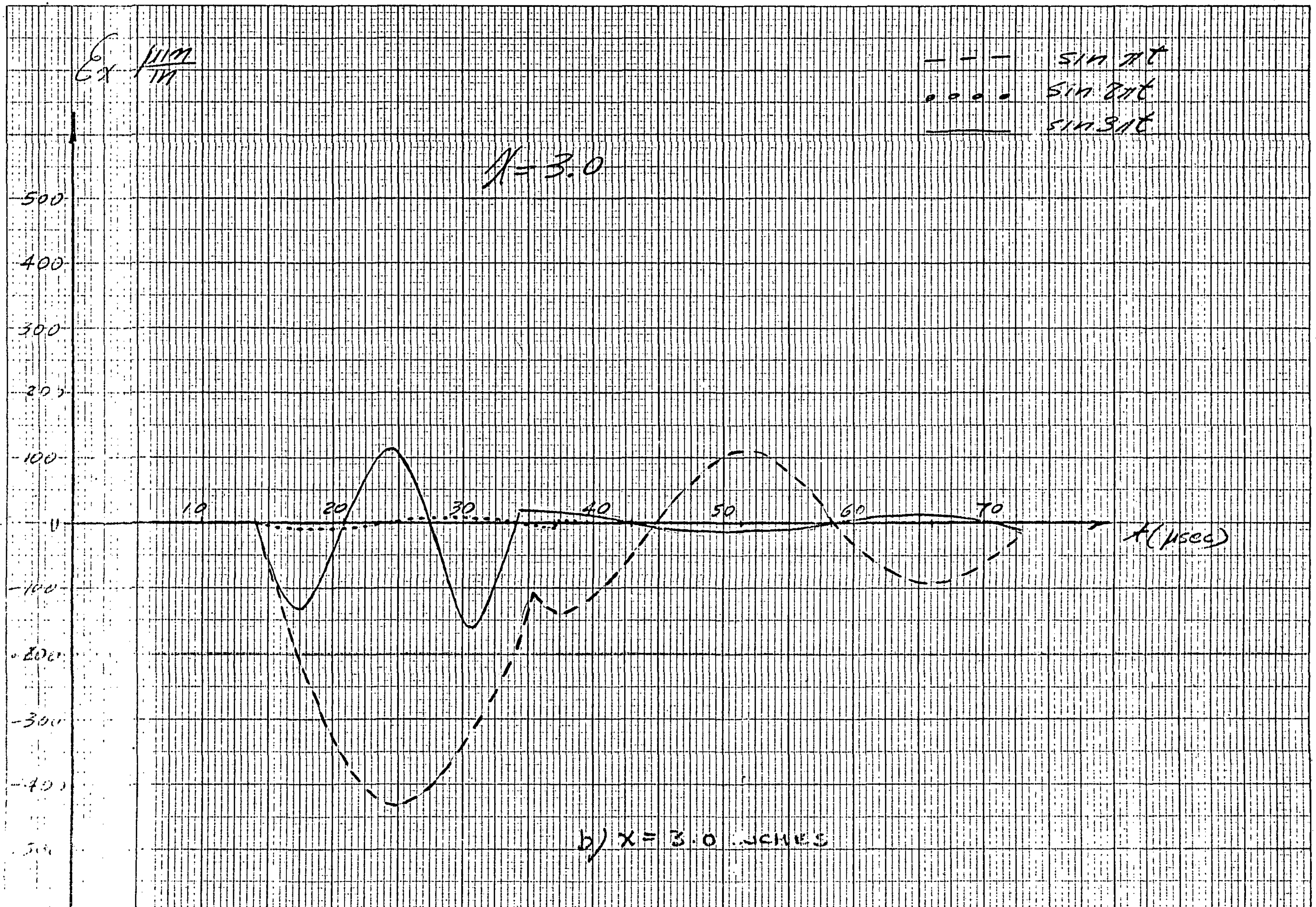

FIGURE 7 - CONT'D

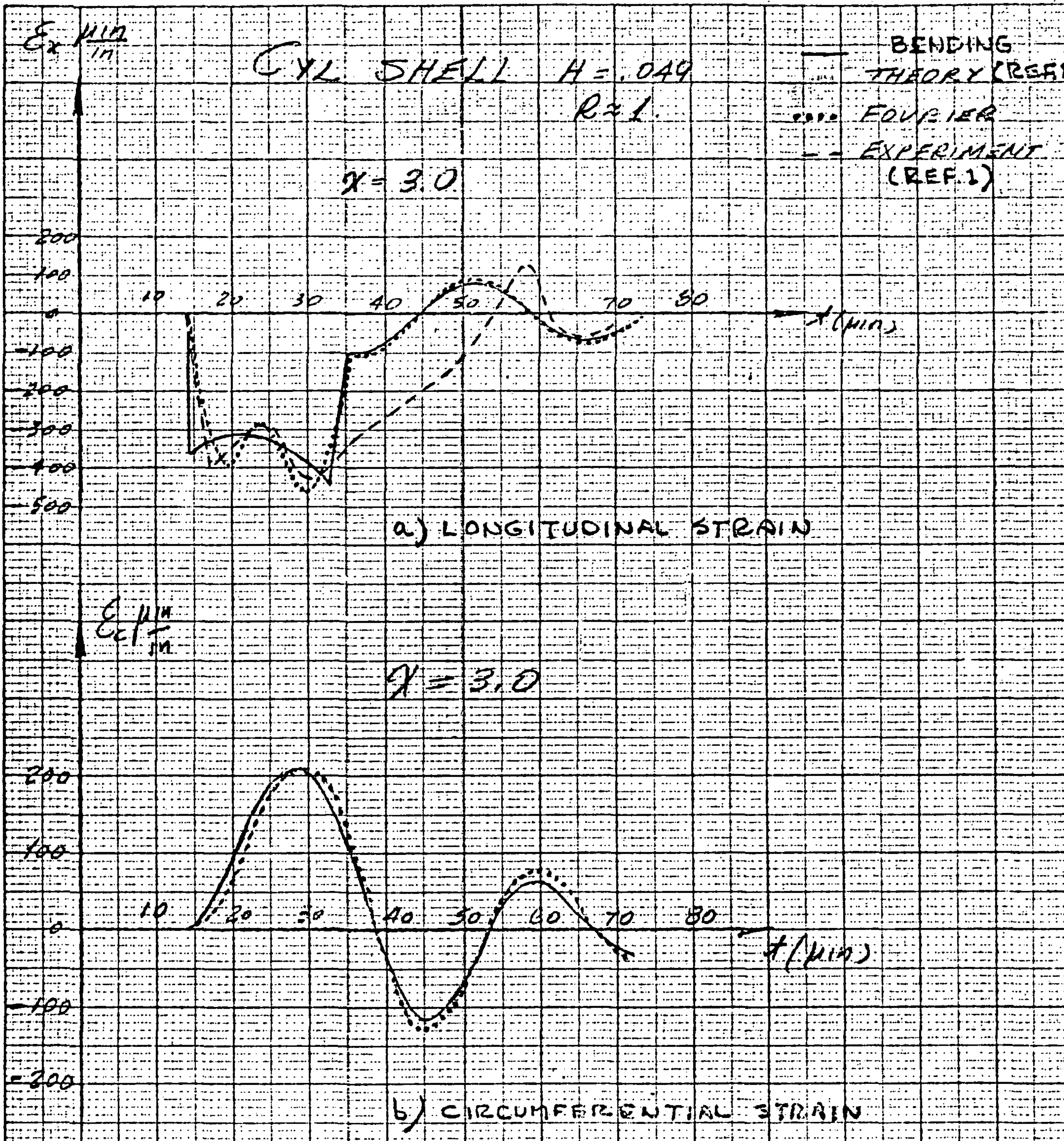

FIGURE 8 COMPARISON OF STRAIN PREDICTIONS

pulse duration. The problem now reduces to determining the effect of the duration of the sine pulse on the transient response of the shell. If this is understood, then by superposition we should be able to determine the effect of an arbitrary pulse's shape and duration on the shell response.

Our first set of runs involved a cylindrical shell (h/R = 0.1) subjected to an axial velocity input of the type

$$\dot{u}(0, t) = \sin \pi \frac{\bar{\tau}}{\bar{\tau}_o} \quad 0 \leq \bar{\tau} \leq \bar{\tau}_o$$

$$N_x(0, t) = 0 \qquad \bar{\tau}_o < \bar{\tau}$$

where $\bar{\tau}_o$ is the pulse duration of the half sine. The remaining boundary conditions at the impacted end were $\bar{Q}_x = M_x = 0$. Transient responses, as predicted by the "bending theory" eq.(A-1), were obtained for values of τ_o such that the inverse of wavelength, $1/\bar{\lambda} = 1/\bar{\tau}_o$ (or in dimensional form $\lambda = t_o c_p$) assumed values of .2, .1, .05, .025, .0167, and .01. In otherwords, the range of the pulse duration was such that the equivalent pulse length varied from being 5 times the thickness to 100 times the thickness. Plots of the longitudinal strain at a location of $\bar{X}$ = 60 are shown in Fig. 9. Comparison of these responses demonstrates an interesting point; the sine pulse disperses less for the long and the short pulse duration than for the intermediate duration. Responses for identical loading conditions were obtained for the classical membrane theory eq. (A-3), the membrane with shear theory eq. (A-2), and the uniaxial theory eq. (A-4). The trends of the longitudinal strain as predicted by the first two of these theories were identical to that of the "bending" theory although there was a slight deviation in magnitude. Of course the uniaxial theory indicated no dispersion across the entire wavelength range since it is governed by the simple wave equation. To illustrate this pulse length effect on the transient response of the cylindrical shell we plotted in Fig. 10 the peak values of the longitudinal strain versus the

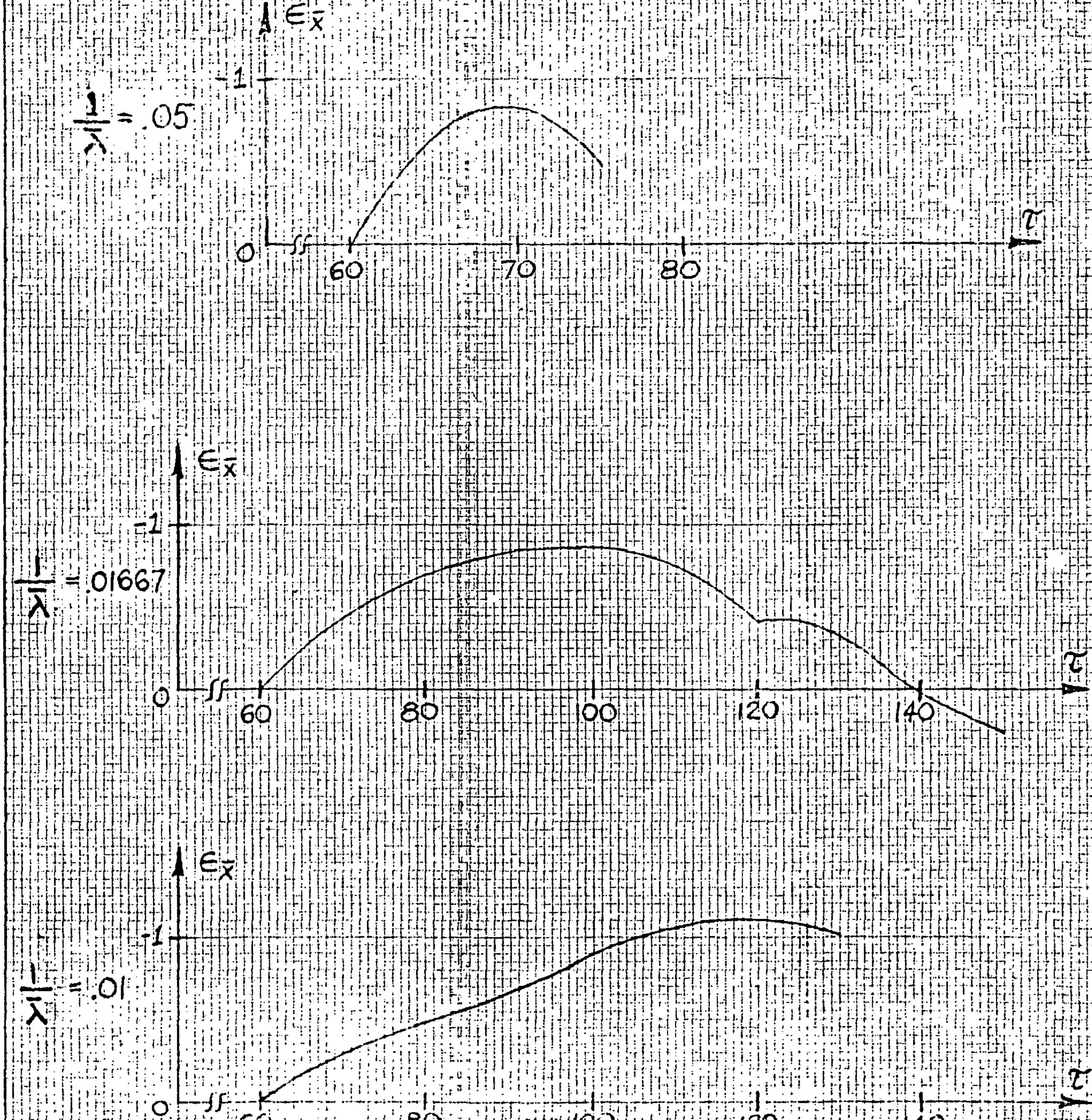

FIGURE 9 RESPONSE OF SHELL TO SINE PULSES OF DIFFERENT PULSE DURATIONS; $\bar{\tau} = 60$

$\frac{h}{\lambda}$ (or $\frac{1}{\bar{\lambda}}$) at the location $\bar{X}$ = 60. A similar plot of this variation for a cylindrical shell with h/R = 0.05 is shown in Fig. 11. This variation of strain with pulse length can be described subjectively as follows: when the wavelength is large ($\frac{h}{\lambda} \to 0$), as compared to the R of the shell, we can consider the wave as seeing a bar and it is well known that for a wave length much larger than the bar radius there exists no dispersion. On the other hand, when the wavelength is smaller than the shell radius and of the order of the shell thickness ($\frac{h}{\lambda} > 0.5$), the wave is seeing essentially a plate. For this case we can understand the lack of dispersion (mathematically) by realizing that the inplane equation of motion (uncoupled from the bending and transverse equations) for a plate is governed by a simple wave equation. The region between these two limits involves coupling between the membrane, radial, and bending modes, thus the dispersion.

The essence of this discussion, as it pertains to understanding the effect of pulse shape and duration on the transient response, is as follows. First, I believe we have demonstrated the importance of pulse duration (equivalent wavelength) on the transient response of a shell. As we have seen, it is the most important parameter to be considered. Second, by using the "building block" approach we can understand the effect the pulse shape will have on the response by simply determining the importance of each of the approximating functions ($\sin \pi t$, $\sin 2\pi t$, $\sin 3\pi t$, etc) for a particular shape via the least square coefficients. Once we know which of these functions is most important we can use curves such as those of Figs. 10 and 11 to determine the magnitude and dispersive nature of each and thus be able to predict the response of actual shape through superposition. This

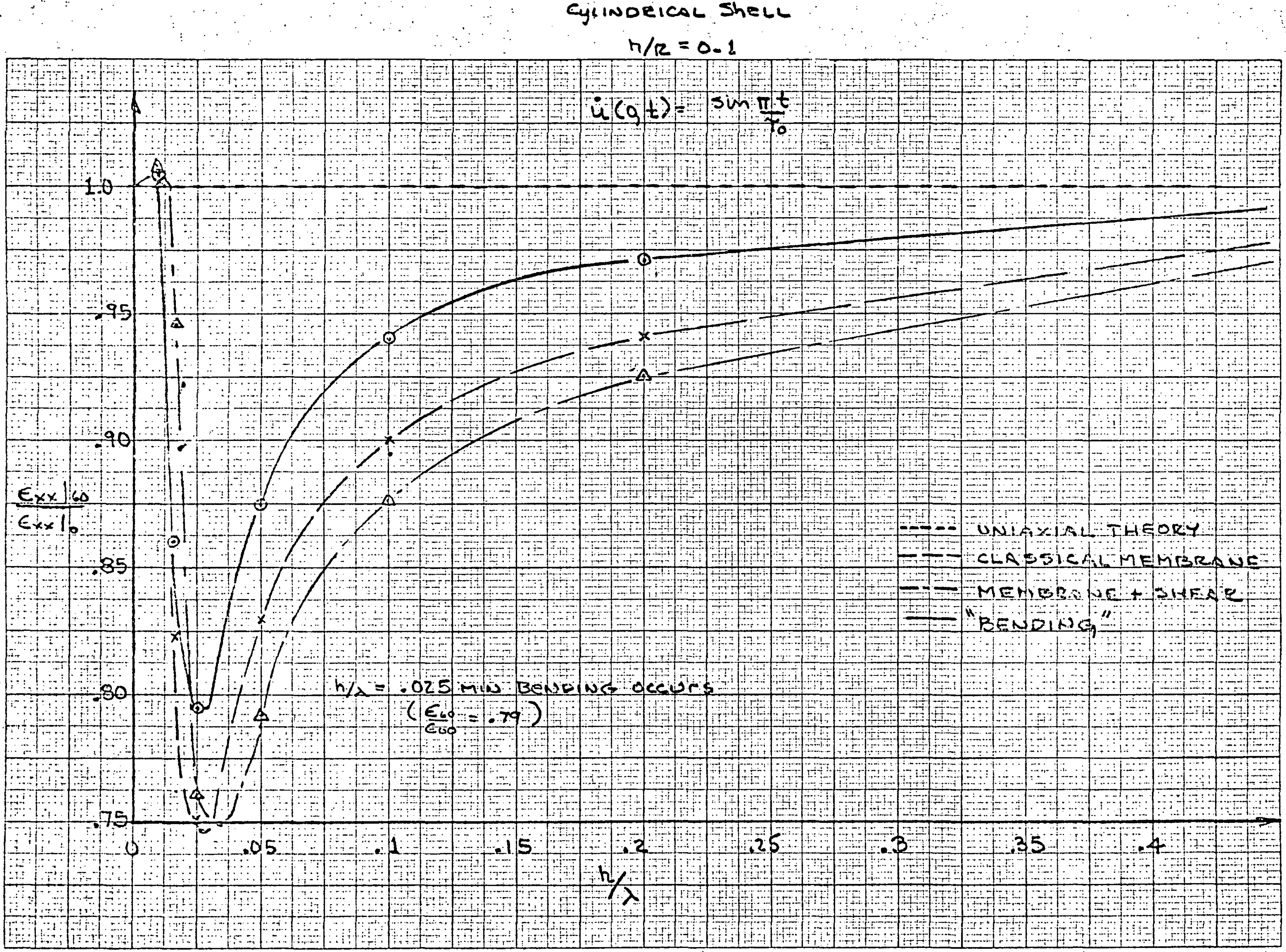

FIGURE 10 STRAIN VS h/λ FOR $h/R = 0.1$

CYLINDRICAL SHELL

$h/R = 0.05$

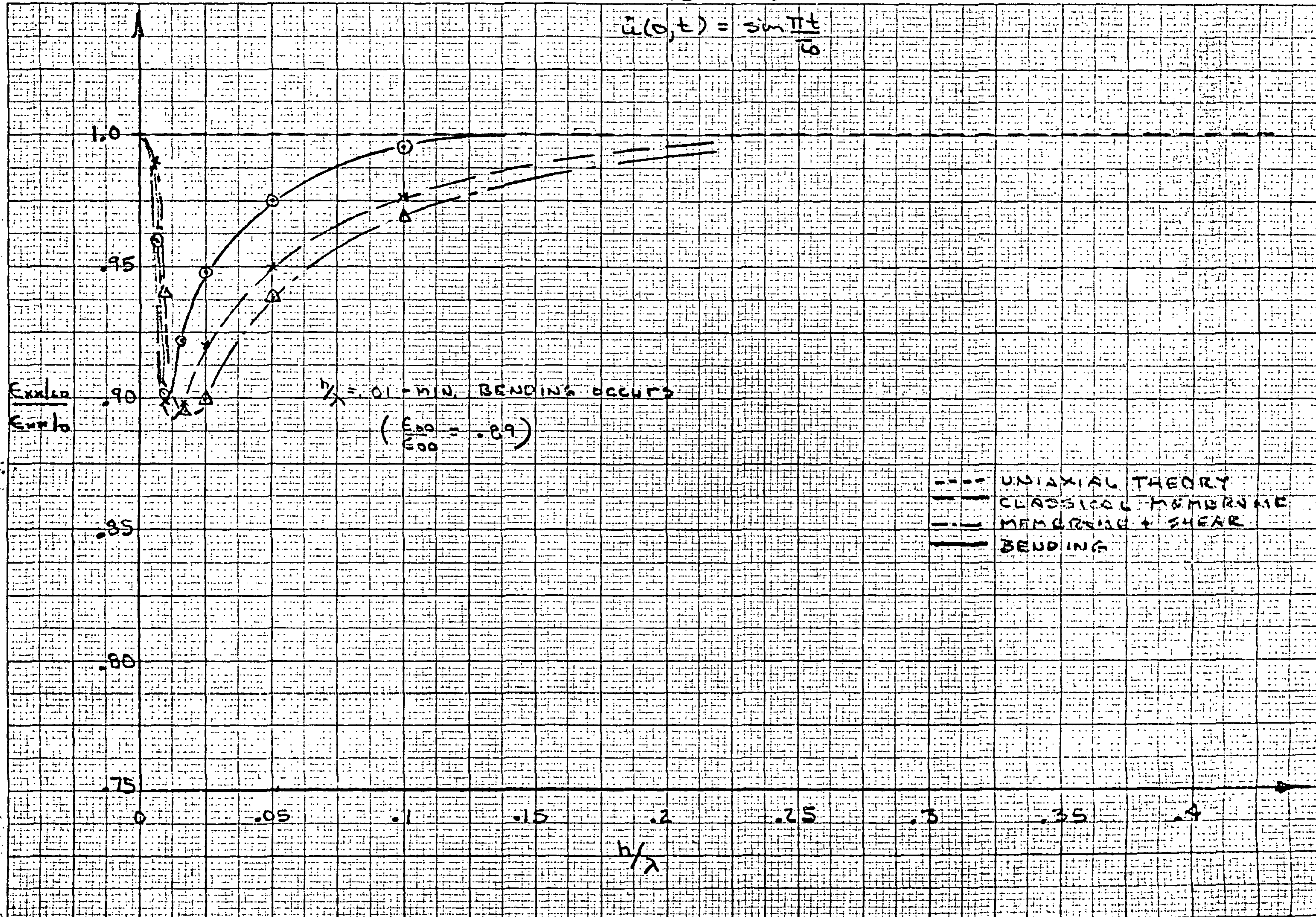

FIGURE 11 STRAIN vs h/λ FOR $h/R = 0.05$

latter point will be discussed in more detail in Section IV where we will compare transient responses as obtained by the "building block" approach and the exact shape approach.

Before concluding this Section, a few points should be mentioned. First, work should be continued along the line of effort just described as I believe this will lead to the understanding of the relationship between dispersion analysis (harmonic) and actual wave propagation. Second, this understanding of the effect of pulse duration on dispersion for single-type pulses has importance in ultrasonic NDT work (see for example Ref. 4).

IV. EFFECT OF PULSE SHAPE ON TRANSIENT RESPONSE OF CYLINDRICAL SHELLS

In this Section of the Report, we demonstrate the importance of the pulse shape (especially the pulse duration) on the transient response of a cylindrical shell. In achieving this goal, we will compute the response of the shell due to the exact shapes used for the loading functions. However, in order to demonstrate the usefulness and importance of our "building block" concept, we will choose certain of these shape responses and compare them with the predictions obtained by this "building block" approach. By doing this, the importance of certain of the pulse shape parameters can be isolated and described. In deciding upon which shapes, specimen properties, and pulse durations to use in these final computations, we relied heavily upon the knowledge gained from the work previously described (e.g. the $\bar{\varepsilon}$ vs h/λ curves of Figs. 10 and 11). This was necessitated by the fact that we could become involved in an endless parametric study with the major results being lost in the massive data. For the sake of clarity and completeness in this Section, certain details previously described in this Report will be briefly repeated.

The two cylindrical shell specimens chosen for our analysis are shown in Fig. 12. Each of these specimens is seen to have a discontinuity in thickness. The reason for this is that a portion of the proposed study pertains to the effect of geometrical discontinuities (the results are discussed in the next Section), so, by analyzing the specimens, as shown, we then have data necessary for the uniform shell and the geometrical discontinuous shell. Notice that for each specimen $L_1/h = 200$, or, the length of the shell to be considered in this Section is 200 times the thickness. The pulse shapes chosen for our study are the same as those shown in Fig. 2. The boundary conditions used were

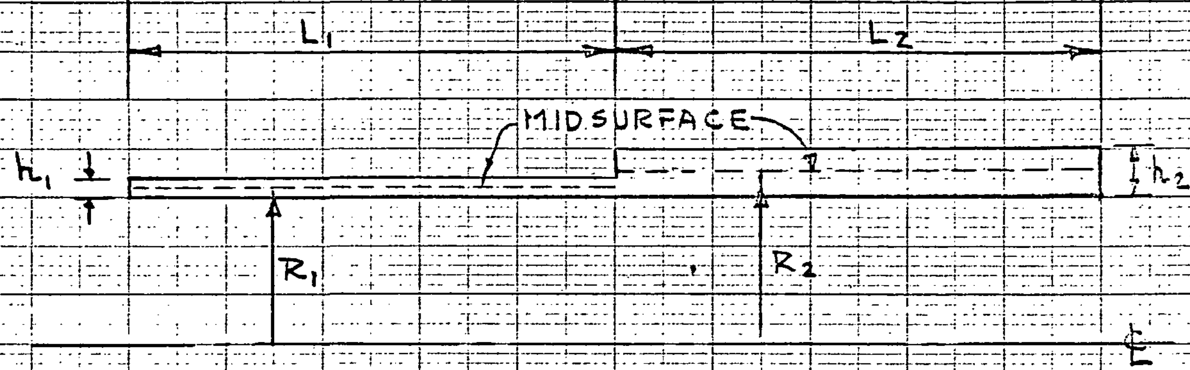

SPECIMEN	h_1	R_1	h_1/R_1	h_2	R_2	h_2/R_2	A_2/A_1	L_1	L_2
#1	.05"	1.0"	.05	.1026"	1.0263"	0.1	2.59	10"	10"
#2	.1026	1.026	0.1	.05	1.0	.05	0.387	20.52"	20.52"

FIGURE 12 SPECIMENS FOR PULSE SHAPE STUDY

$$\begin{cases} \dot{\bar{u}}(0,t) = 1 \times \text{shape function}; & 0 \leq \bar{\tau} \leq \bar{\tau}_0 \\ \bar{N}_x(0,t) = 0 & ; \quad \bar{\tau}_0 < \bar{\tau} \end{cases}$$

and

$$\bar{M}_x(0,t) = \bar{Q}_x(0,t) = 0$$

and the initial conditions were zero. Note that these boundary conditions were all applied at the left end of the specimens as shown in Fig. 12. Finally, the equations used for the analysis were those of the bending theory (eqs. A-1) since we have seen (Figs. 10 and 11) that, except for the uniaxial theory, there is no sizeable discrepancy between the predictions of the bending theory with those of the modified membrane theory or the classical membrane theory. We should remember two points here. First, the uniaxial theory will yield a transient response in which there is no change in shape or magnitude of the pulse as it propagates along the shell and second, the fact that there is only a slight difference between the predictions of the other theories applies because we are only considering longitudinal loadings; this is not true for radial loadings.

The first set of computations involved specimen #1 for which $h_1/R_1 = 0.05$. Observation of Fig. 11 shows us that for the pulse shapes having a value of $1/\bar{\lambda} = h/\lambda = 0.05$ we should not expect much shape change or dispersion as the wave traverses the shell. In order to reach this conclusion we are relying on our sine "building block" concept when using Fig. 11. Recall that each of the exact shapes can be approximated by a series of sine pulses, the first sine term having a pulse duration equal to the exact shape pulse duration. The second and higher terms of the sine series will have pulse durations (or λ's) which are shorter, thus, will have even less dispersion because we are moving to the right on Fig. 10 (e.g. the third term will have a value of

h/λ of 0.15). On the other hand, by observing Fig. 11 we would expect pulse shapes having a pulse duration equivalent to $h/\lambda = 0.01$ to suffer much dispersion. With these predictions established from Fig. 11, we then ran two sets of computer calculations; the first, shown in Fig. 13, are the results for the shapes having a pulse duration equivalent to $h/\lambda = 0.05$ and the second, shown in Fig. 14, the results for $h/\lambda = 0.01$. In Figs. 13 and 14 we have plotted the longitudinal strain at $\bar{x} = 50, 100,$ 150 and 300; remember that the location $\bar{x} = 300$ is beyond the geometrical discontinuity, so, the strain history at this location will not be discussed until the next section as it represents the transmitted wave through the discontinuity. Observation of Fig. 13 and 14 confirms our predictions from Fig. 11. For example, in the case of $h_1/\lambda = 0.05$ we note very little change in shape, pulse duration, or magnitude as the wave propagates down the shell; the peak magnitude of the isoceles triangle pulse at $\bar{x} = 150$ is 0.91. On the other hand, we see for the case of $h_1/\lambda = 0.01$ the pulse changing shape, increase of pulse duration, and more attenuation of peak magnitudes; the peak magnitude of the isosceles triangle pulse at $\bar{x} = 150$ is now 0.75.

The second set of computations involved specimen #2 for which $h_1/R_1 =$ 0.10. Observation of Fig. 10 shows us that more dispersion is possible for this h/R ratio than in the previous case. For this specimen, then, we performed three sets of computations; these were for the values of h_1/λ of 0.1, 0.025, and 0.01. We would predict, based on Fig. 10, that the pulse duration causing the least dispersion of the pulse would be for those pulse shapes having $h_1/\lambda = 0.1$, while the most dispersive would be for $h_1/\lambda = 0.025$; the pulse shapes having $h_1/\lambda = 0.01$ should lie between these two. Figs. 15, 16, and 17 are the results of the computer calculations for values of h_1/λ of 0.01, 0.025, and 0.1, respectively. Observation of Figs. 15, 16 and 17

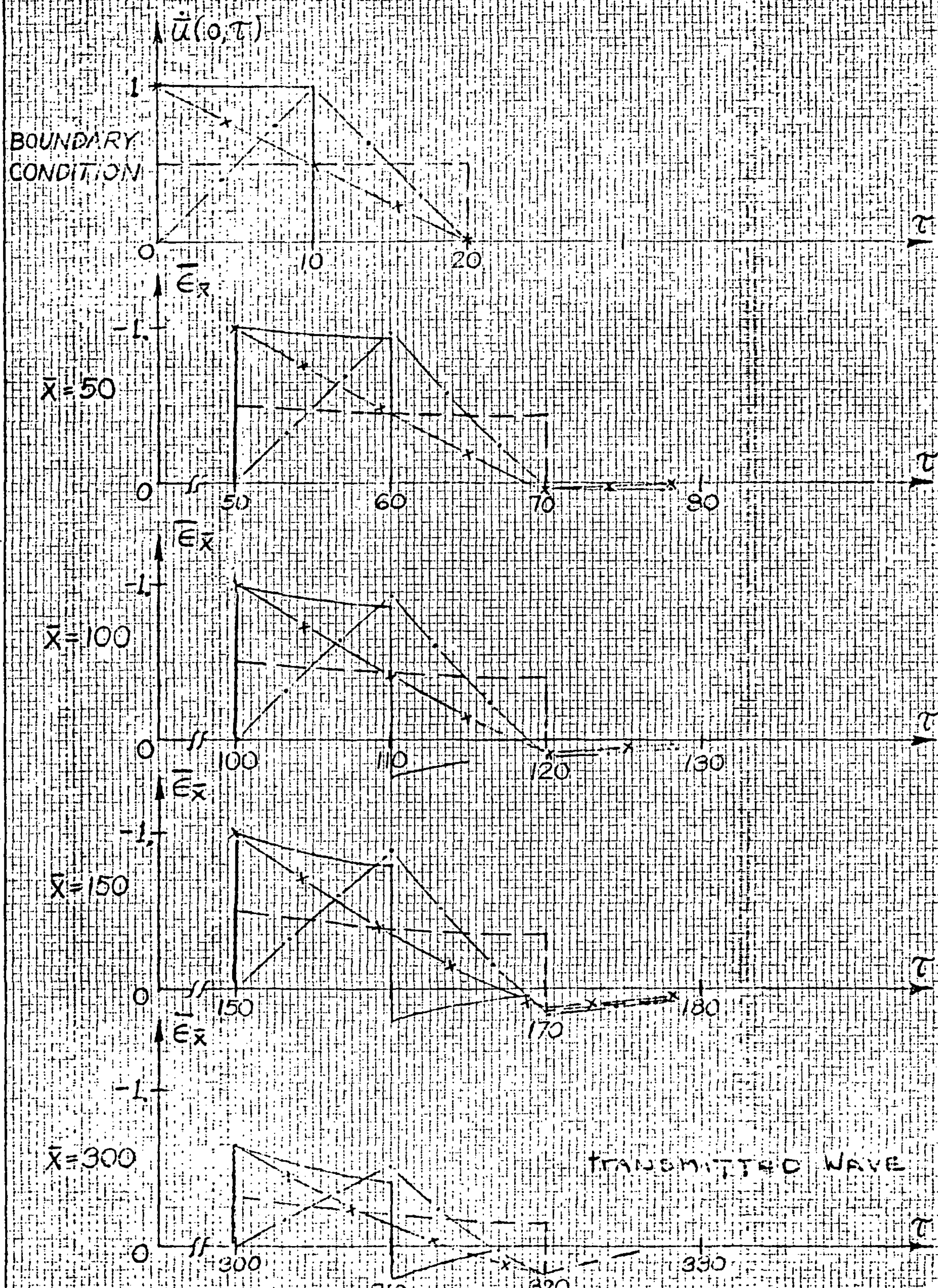

FIGURE 13 LONGITUDINAL IMPACT OF SPECIMEN 1 $(\frac{h}{R_1}=.05)$ AT SMALL END; $h/\lambda = 0.05$

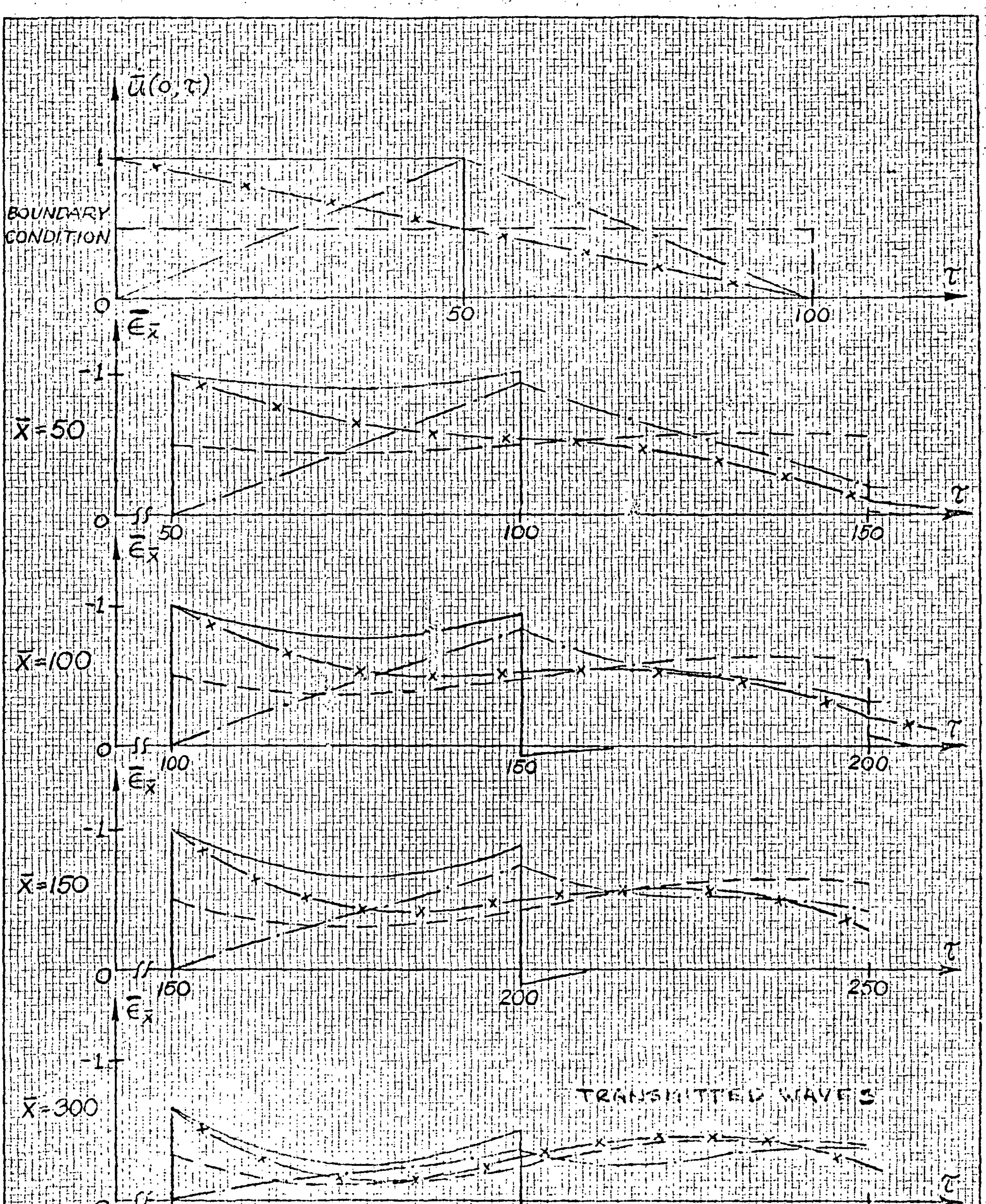

FIGURE 14 LONGITUDINAL IMPACT OF SPECIMEN 1 ($\frac{h_1}{R_1}$ = .05) AT SMALL END, $h_1/\lambda = 0.01$

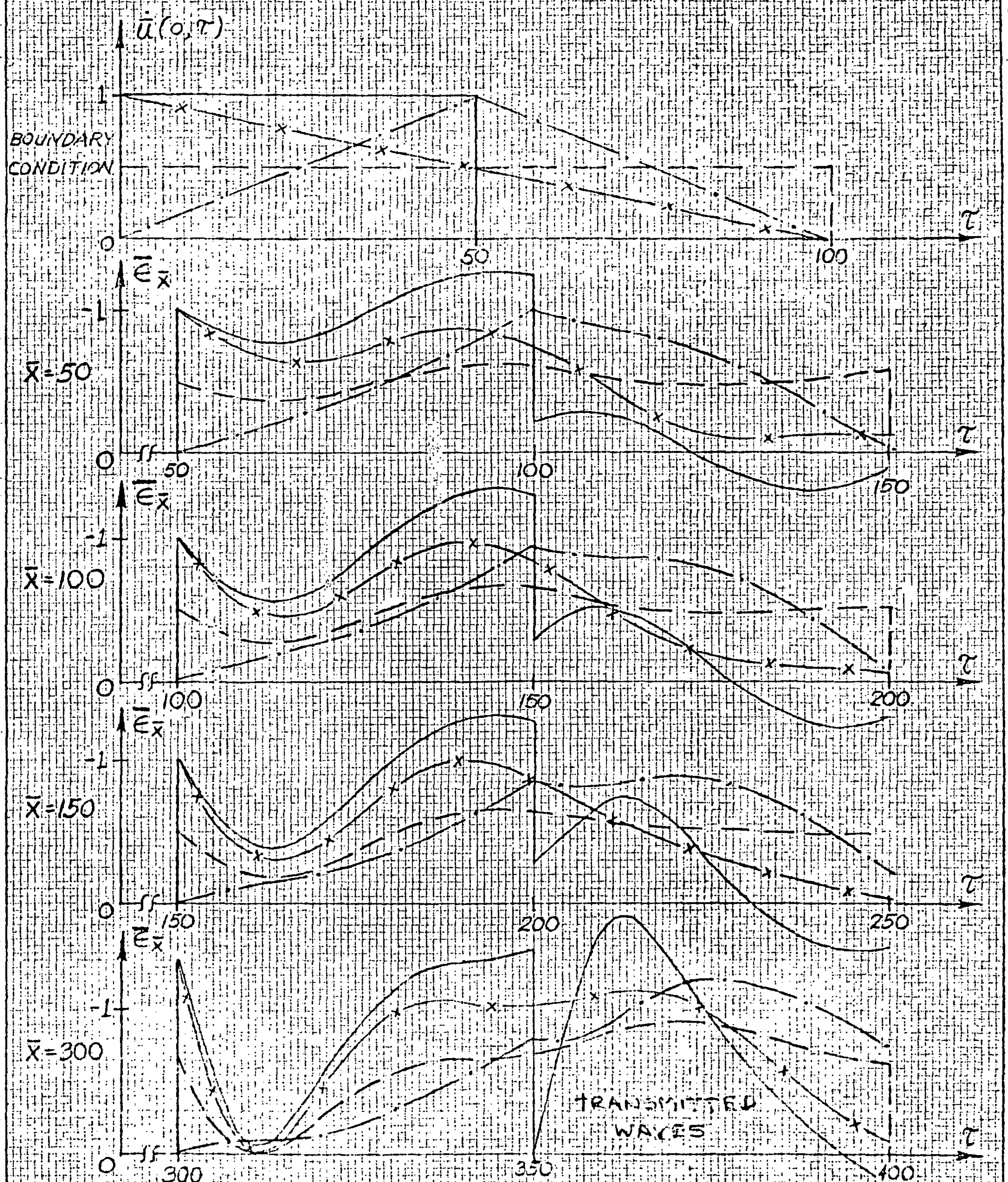

FIGURE 15 LONGITUDINAL IMPACT OF SPECIMEN 2 $\left(\frac{h_1}{R_1}=0.1\right)$ AT LARGE END, $h_1/\lambda = 0.01$

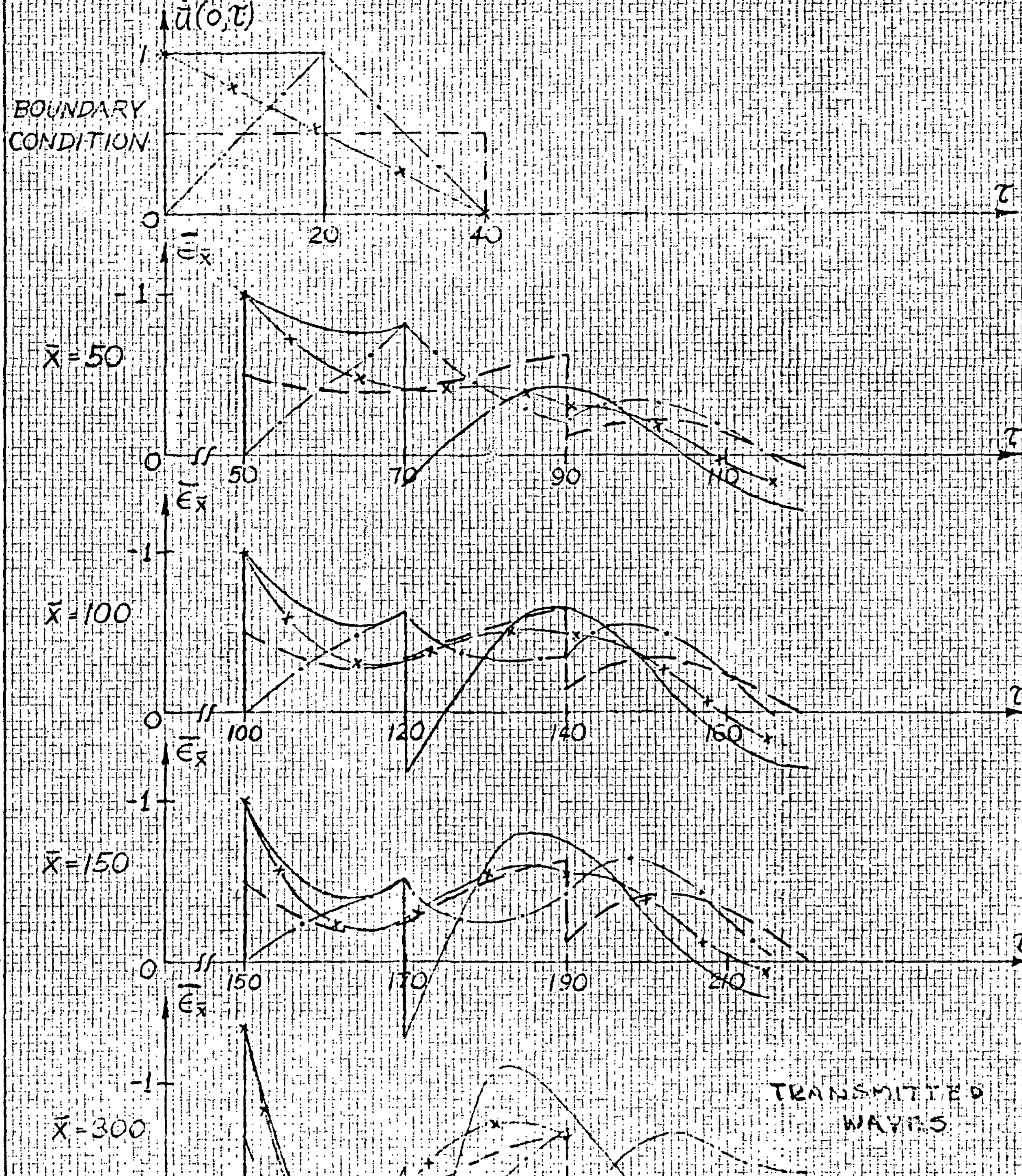

FIGURE 16 LONGITUDINAL IMPACT OF SPECIMEN 2 ($\frac{h_1}{R_1}=0.1$) AT LARGE END, $h_1/\lambda = 0.025$

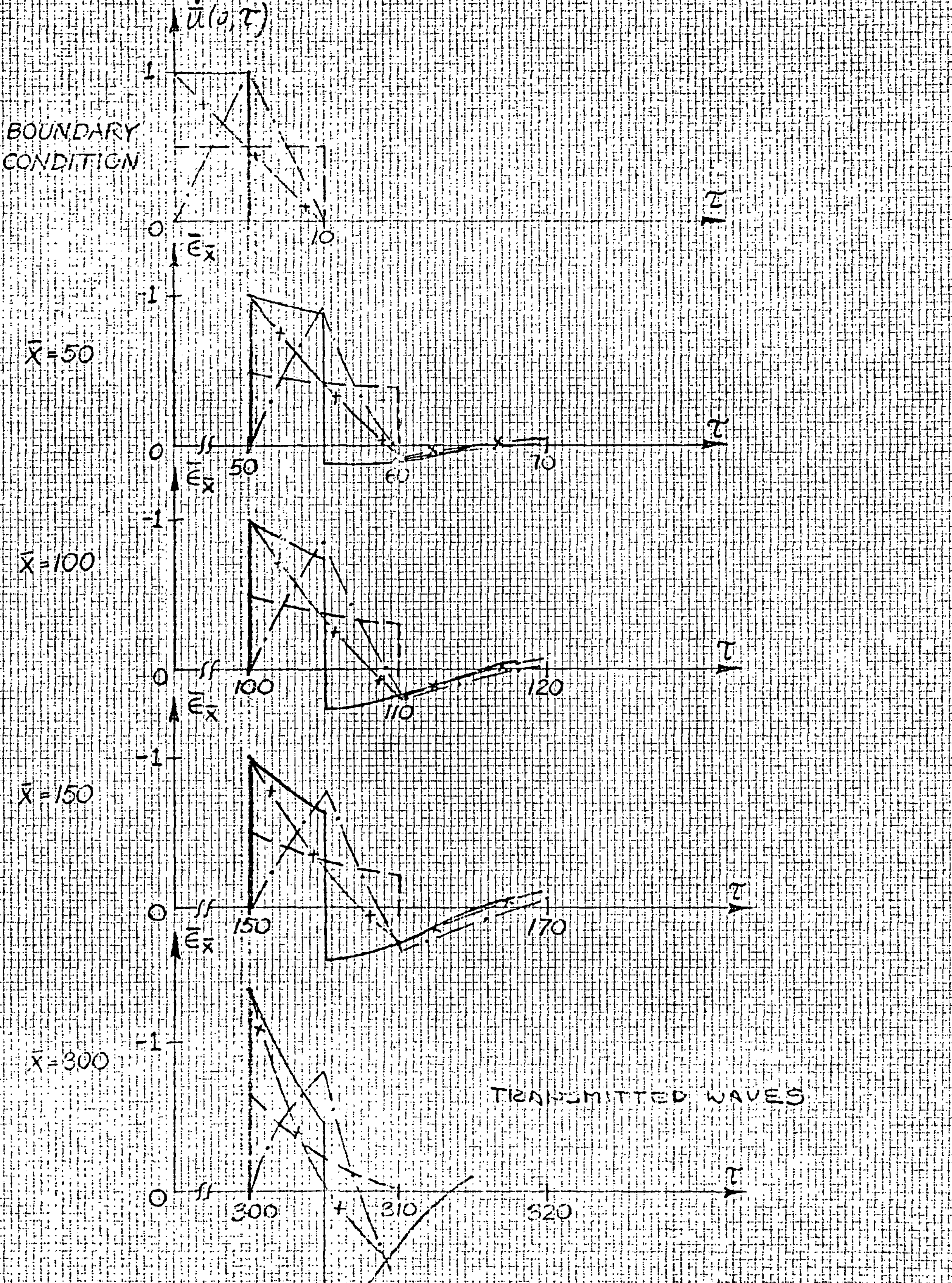

FIGURE 17 LONGITUDINAL IMPACT OF SPECIMEN #2
AT LARGE END, $h/\lambda = 0.1$

indeed confirms our predictions. The pulse shapes with $h_1/\lambda = 0.1$ did not change shape drastically, maintained essentially the same pulse duration and had a peak value for the isosceles shape of 0.8 at $\bar{x} = 150$. The pulse shapes with $h_1/\lambda = 0.01$ did change shape some what, increased in pulse duration, and had a peak value for the isosceles shape of 0.85 at $\bar{x} = 150$. Finally, the results for the $h_1/\lambda = 0.025$ show a much more drastic shape change and increase in pulse duration than either of the previous two cases; the peak value for the isosceles triangle has diminished to a value of 0.65. Note, also, from these Figures that the longer pulse duration pulses lose their identity in shape and begin to resemble one another in shape as the wave propagates along the shell. This indicates that for long duration pulses the present practice of not worrying about the shape of the initial pulse in detail is most likely proper for practical applications.

The results of this study indicate that the pulse shape parameter which effects the transient response of a cylindrical shell is the parameter h/λ which is directly related to the pulse duration, τ_0, through the relation $\lambda = \tau_0 \, c_p$. We have shown that the degree of dispersion of a pulse is related to this ratio. A useful tool in predicting whether a particular pulse will be dispersive is the type of curves shown in Figs. 10 and 11. In order to demonstrate the usefulness of the "building block" concept to actually predict the transient response of the shell subjected to a particular shaped pulse, we will compute the transient response of specimen #2 due to the isosceles shaped pulse by this technique. We will use the two term approximation of the isosceles shape as shown in Fig. 5; in otherwords

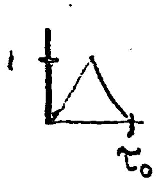

$$\cong \quad 0.81099 \sin \pi \frac{\tau}{\tau_0} - .09048 \sin 3\pi \frac{\tau}{\tau_0}$$

We will perform the calculations for this isosceles shaped pulse for the cases of $h_1/\lambda = 0.025$ and 0.01. The first step is to compute the response of the shell to each of the sine functions. Next, we superimpose the results by use of the previous equation and we have the resulting approximations for the transient response of an isosceles shapes pulse. Figs. 18 and 19 contain the results of the "building block" response predictions for $h_1/\lambda = 0.025$ and $h_1/\lambda = 0.01$, respectively. These Figures each contain the response to the sine functions, the superimposed response, and the response due to the actual shape. Comparison of the response predictions as obtained by the exact shape and the approximation, show that the "building block" concept can be used not only for subjective predictions, but, also practical predictions. Once we understand the way in which individual sine pulses effect the transient response of a shell we can superimpose and understand the response due to an arbitrary shaped pulse.

In conclusion, we must say that an experimental program to verify these analytical results is warranted; the reason being that we are solving a system of approximate (although inclusive) governing differential equations for the shell response. An experimental verification of the curves shown in Figs. 10 and 11 would be sufficient to verify our results.

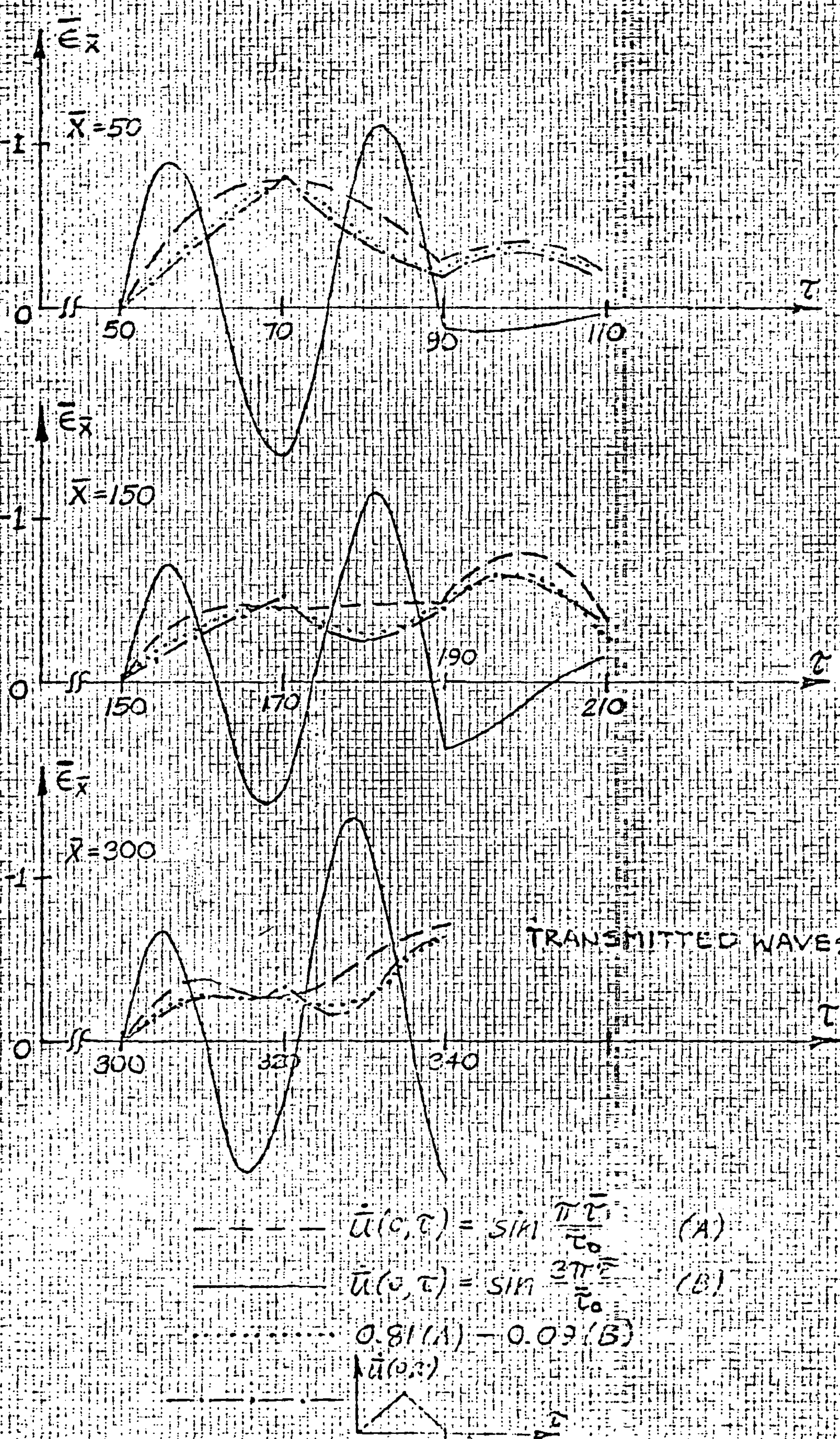

FIGURE 19 TRANSIENT RESPONSE BY SUPERPOSITION FOR $h_1/\lambda = 0.025$; $h_1/R_1 = 0.1$

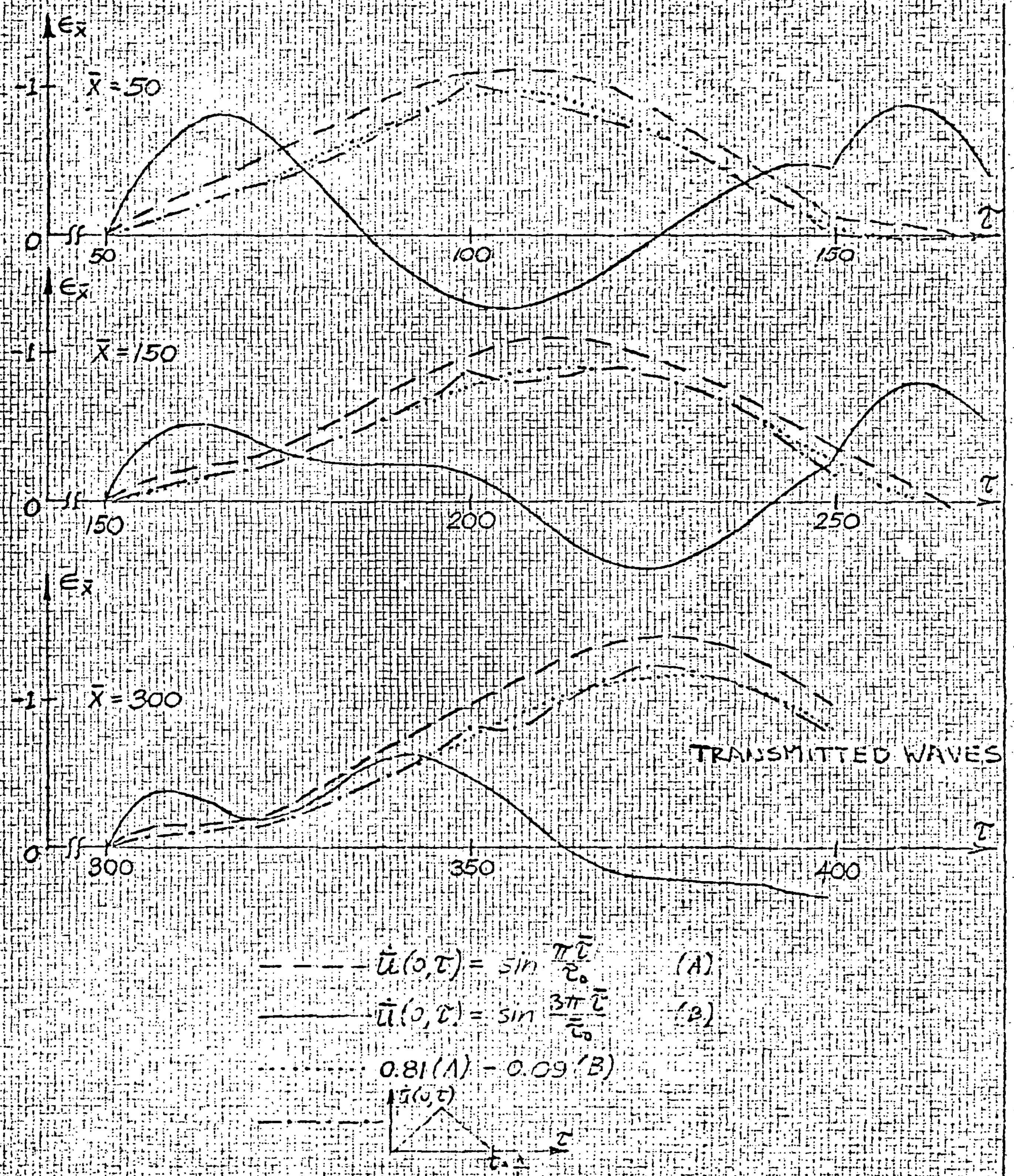

FIGURE 19 TRANSIENT RESPONSE BY SUPERPOSITION FOR $h_1/\lambda = 0.01$; $h_1/R_1 = 0.1$

V. EFFECT OF PULSE SHAPE ON TRANSIENT RESPONSE OF CYLINDRICAL SHELLS HAVING GEOMETRICAL DISCONTINUITIES

The purpose of this phase of the research program is to determine the effect of pulse shape on the transient response of a cylindrical shell with a geometrical discontinuity subjected to a longitudinal impact. In this Section we will be referring to Figs. 13 through 19, again, as was mentioned previously. In particular, we will be interested in the strain responses at $\bar{x}$ = 150 and 300 in these Figures. The strain histories at these two locations can be considered as the incident and transmitted pulses, respectively. Observation of Figs. 13 and 14 for specimen #1 and Figs. 15, 16, and 17 for specimen #2 establishes certain trends:

1. For the shorter pulse duration the actual shape is important in establishing the peak transmitted pulse magnitude. For example, observation of Fig. 17 demonstrates that the maximum magnitude is established by initial rise time.
2. For the longer pulse duration the shape does not play as important a role as for the shorter duration pulses. For example, the peak magnitudes of the transmitted pulses, as shown in Fig. 15, are not dependent upon the rise time or shape parameters. As a matter of fact, we see in this figure that the peak magnitudes occur well behind the wave front and that the deviation between these magnitudes is not as large as that which occurs for the shorter duration pulse. Note, also, in Fig. 15 that the pulses have essentially lost their identity and in fact are quite similar behind the wave front.

3. No discernible "rule of thumb" formula seems to be appropriate for the prediction of transmitted to incident strain or stress ratios. For the shorter pulses having a short rise time the simple uniaxial equation (Ref. 5)

$$\frac{[\varepsilon_x] \text{ transmitted}}{[\varepsilon_x] \text{ incident}} = \frac{2A_1}{A_2+A_1}$$

would yield reasonable results, but, for the pulses with either long rise times or long pulse duration it appears that a complete computer analysis is necessary.

VI. EXPERIMENTAL MEASUREMENT OF SHEAR WAVE VELOCITY IN A CYLINDRICAL SHELL UNDER RADIAL IMPACT

Another phase of research initiated under this grant was that of developing an experimental technique for generating and measuring shear pulses in a cylindrical shell. The motivation for this study was to develop an experimental capability which when combined with our analytical capability would equip us with the necessary tools to better understand the role of shear waves in the transient response of shells. Following is a brief description of this phase of our research effort.

Experimental studies of propagation of shear wave in cylindrical shells are not found in the literature. Some investigators [6,7] studied shear wave velocity utilizing the ultrasonic techniques. Steveninck [8] developed apparatus for simultaneous determination of longitudinal and shear wave in porous media under pressure. He demonstrated the problem of separating the longitudinal and shear wave. The oscilloscope traces obtained in [8] demonstrated the difficulty in obtaining a clear strain pulse which propagates with the shear velocity. Ref. [9] shows some typical oscilloscope traces in the study of radiation from an explosion in a circular disk.

In this section a technique to measure shear wave velocity in a cylindrical shell under radial impact is developed. The concept for generating the shear wave was as follows (see Fig. 20). An explosive is mounted inside a plug which fits into the end of the shell. The explosive is detonated resulting in a pulse propagating radially outward from the center. The pulse then induces into the end of the shell a radial loading thus generating the shear wave. The radial impact is obtained by an explosion of an electrical detonator inserted in plexiglass and in lexan plugs.

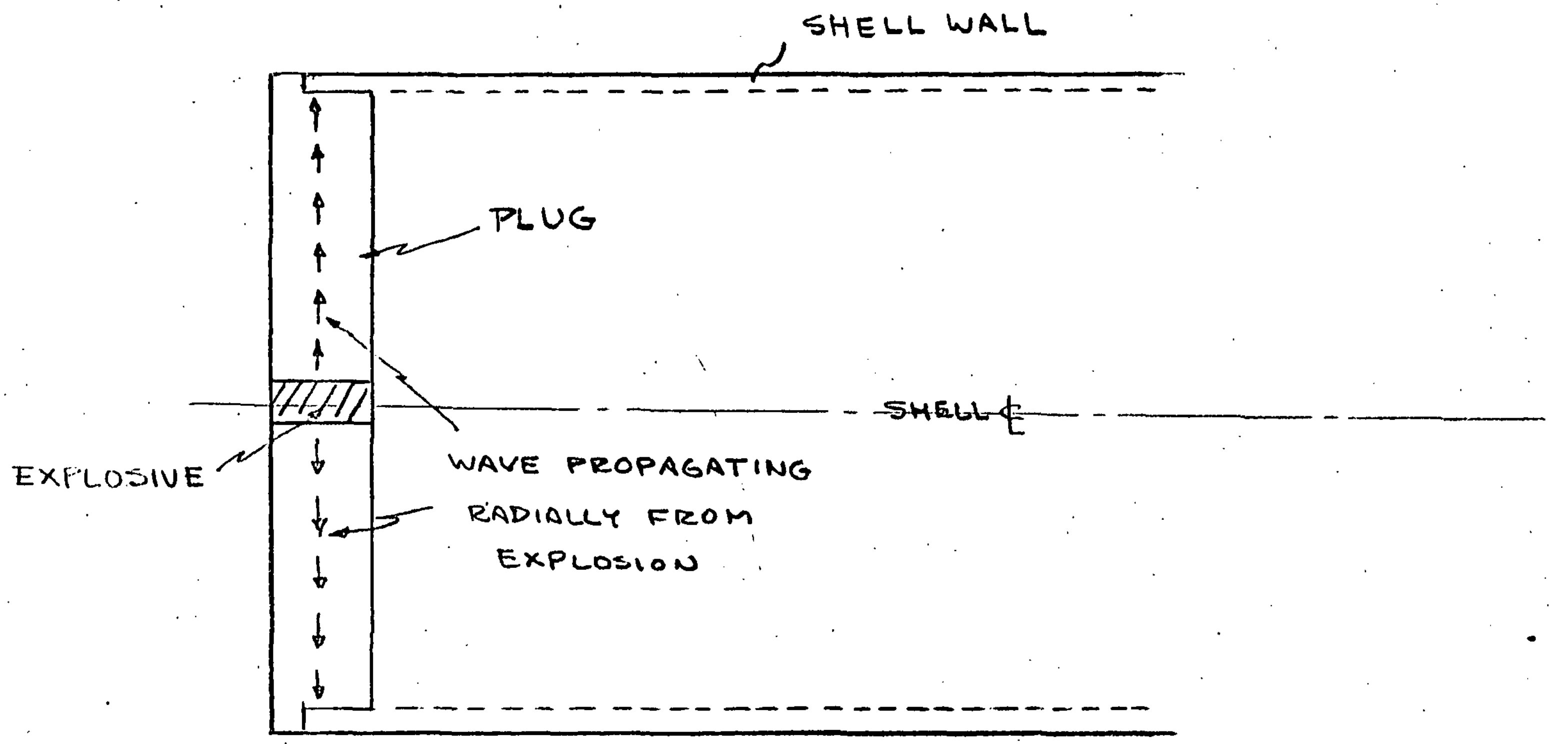

FIGURE 20   SCHEMATIC OF SHEAR WAVE GENERATION

The purpose of using plexiglass or lexan was to slow down the wave initiated by the explosion in order that we will obtain a symmetrical wave in the aluminum cylindrical shell. A symmetric wave will eliminate the effect of bending and thus produce a cleaner strain pulse propagating with the shear velocity.

Strain gages mounted on the outside surface at various axial locations of the shell were used to obtain oscilloscope traces; from which the shear velocity is determined. However, observation of the oscilloscope traces show the presence of a precursor bending wave propagating at the plate velocity.

EXPERIMENTAL PROCEDURE

A straight cylindrical shell fabricated from 6061-T6 aluminum was radially impacted by an explosion of an electrical detonator embedded in plexiglass and lexan plugs. Average properties for the aluminum are

$E = 9.78 \times 10^6$ psi = Young's modulus of elasticity

$\nu = 0.33$ = Poisson's ratio

$c_p = 214,500$ in/sec. = Analytical plate velocity = $[E/\rho(1-\nu^2)]^{1/2}$

$c_s = 113,338$ in/sec. = Analytical shear velocity = $K(G/\rho)^{1/2}$

The geometrical properties of the shell are shown in Fig. 21.

Two types of electrical detonators were used. The first was the Du Pont X-549 R electrical detonator. This type of electrical detonator has a slow firing time of about 1 millisecond and has 0.3 grams HMX base charge. To avoid any electrical noise and current the detonator wires were shielded and grounded. In addition the aluminum cylindrical shell was grounded, which helps in obtaining more clear oscilloscope traces.

Several designs of plexiglass plugs were used and the final one used is shown in Fig. 22. The use of a plexiglass as a transmitter of the wave to the aluminum shell was advantageous in trying to obtain a symmetrical

Table 1. - Specimen Specifications

Specimen Number	h(in.)	h/R	E(lb/in^2)	ρ(lb/ft^3)	Cp($\frac{ft}{sec}$)
1	.049	.052	10.34×10^6	170.27	17,767
2 (T-13)	.125	.133	9.78×10^6	170.27	17,281
3	.250	.286	10.25×10^6	170.27	17,674

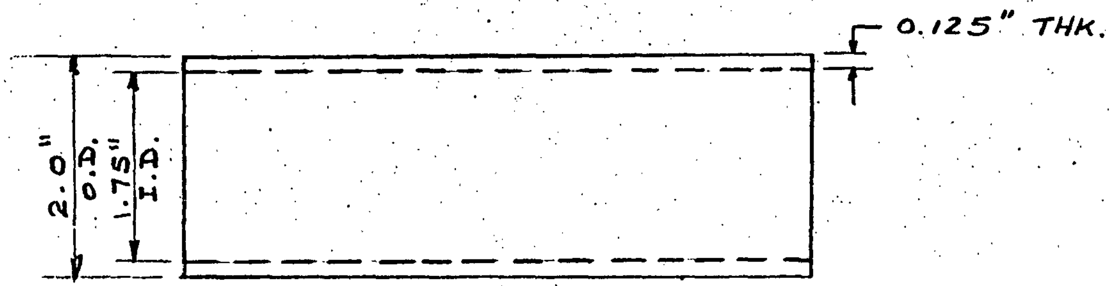

SPECIMEN T-13

FIGURE 21 PROPERTIES OF SHELL

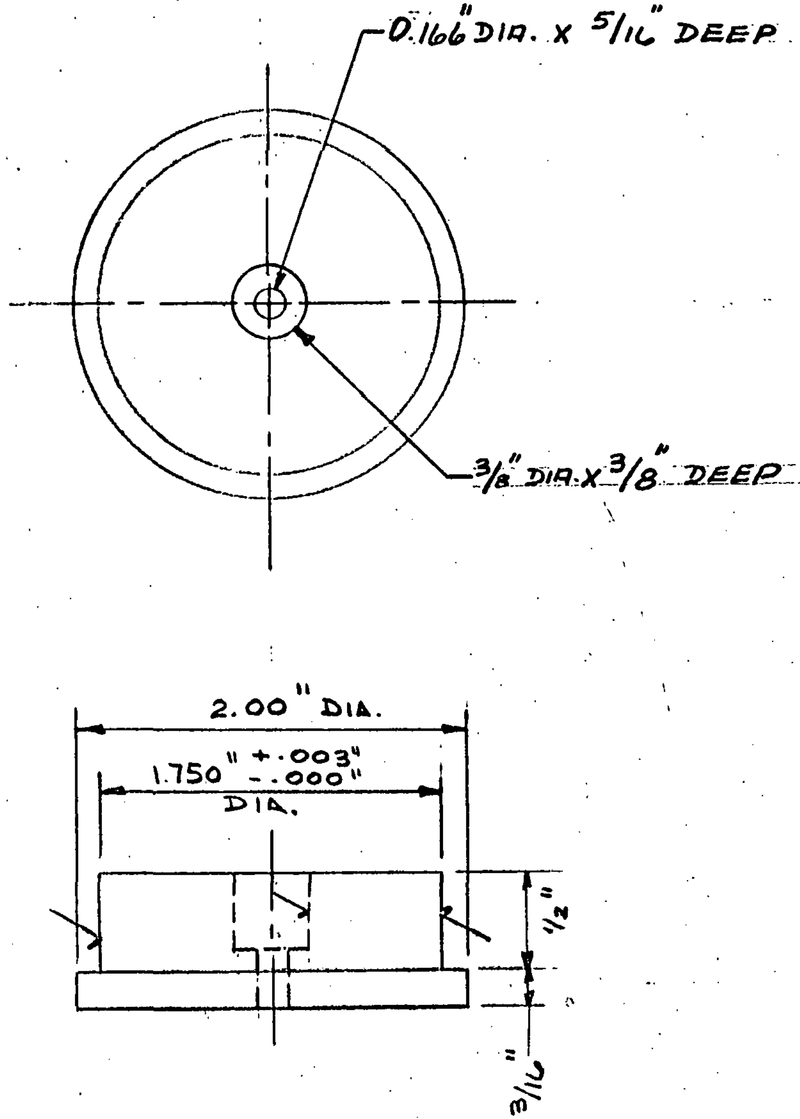

FIGURE 22 - PLEXIGLAS

SPECIMEN T-13

SCALE: FULL SIZE

DWG. SUPERCEED PREVIOUSE DWG. 9/2/71

wave, since the wave in plexiglass travels slower than in the aluminum. For each explosion a new plug was used, since damage did occur to the plug after the explosion.

A second type of electrical detonator used was the Du Pont X-811D miniature conductive mix detonator. This type of detonator has a faster rise time of 4-8 microseconds, and has 52 mg of explosive. There are no wires in this type of detonator and the problem of interferences was reduced. The fast firing time will enable us to obtain better oscilloscope traces. Since this type of detonator has more explosive, it was embedded in a lexan plug which is stronger and more resistant to impact. The basic design of the lexan plug was similar to the plexiglass plug. However, since the X-811D detonator are also smaller than the first type the lexan could be shortened and we could thus obtain a better impact condition at the aluminum shell. The lexan plug is shown in Fig. 23.

Micromeasurement strain gages, 1/8 inch long, are mounted on the outside surface of the shell at various axial locations, as shown in Fig. 24. Ellis BAM-1B bridge amplifiers tuned to a frequency response of 100 KHZ are used to provide proper calibrated strain scaling of the oscilloscope. A trigger gage located near the impacted end was used to trigger the scope. Three alignment gages mounted on the outside surface 120 deg. apart were used to assure asimultaneity of impact, however in our testing only two gages were used. The arrival time of the propagating pulse at the various gage locations is obtained from the oscilloscope trace; since the distance between strain gages is known the velocity of propagation of the strain pulse is obtained by

$$V = \frac{x}{t}$$

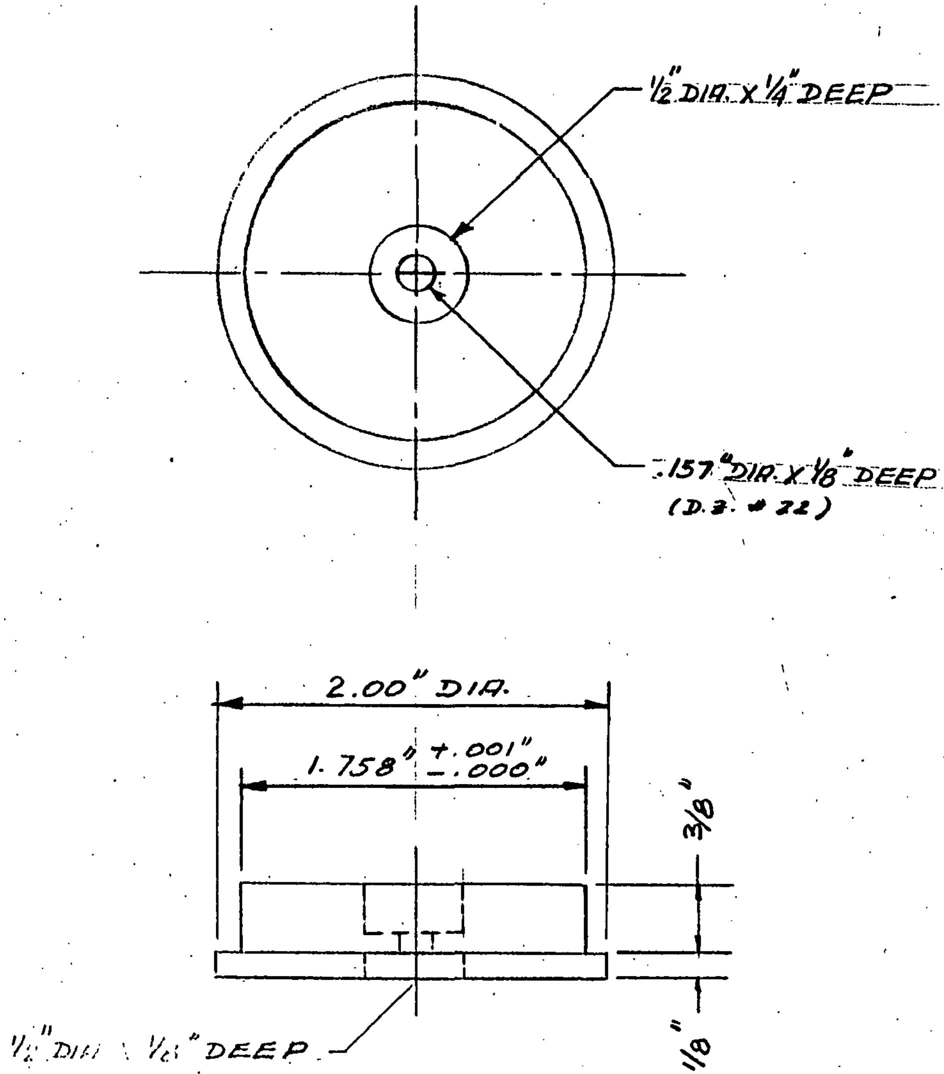

FIGURE 23- LEXAN

SCALE: FULL SIZE

DRAWN: A. BLUM
DATE: 11/5/71

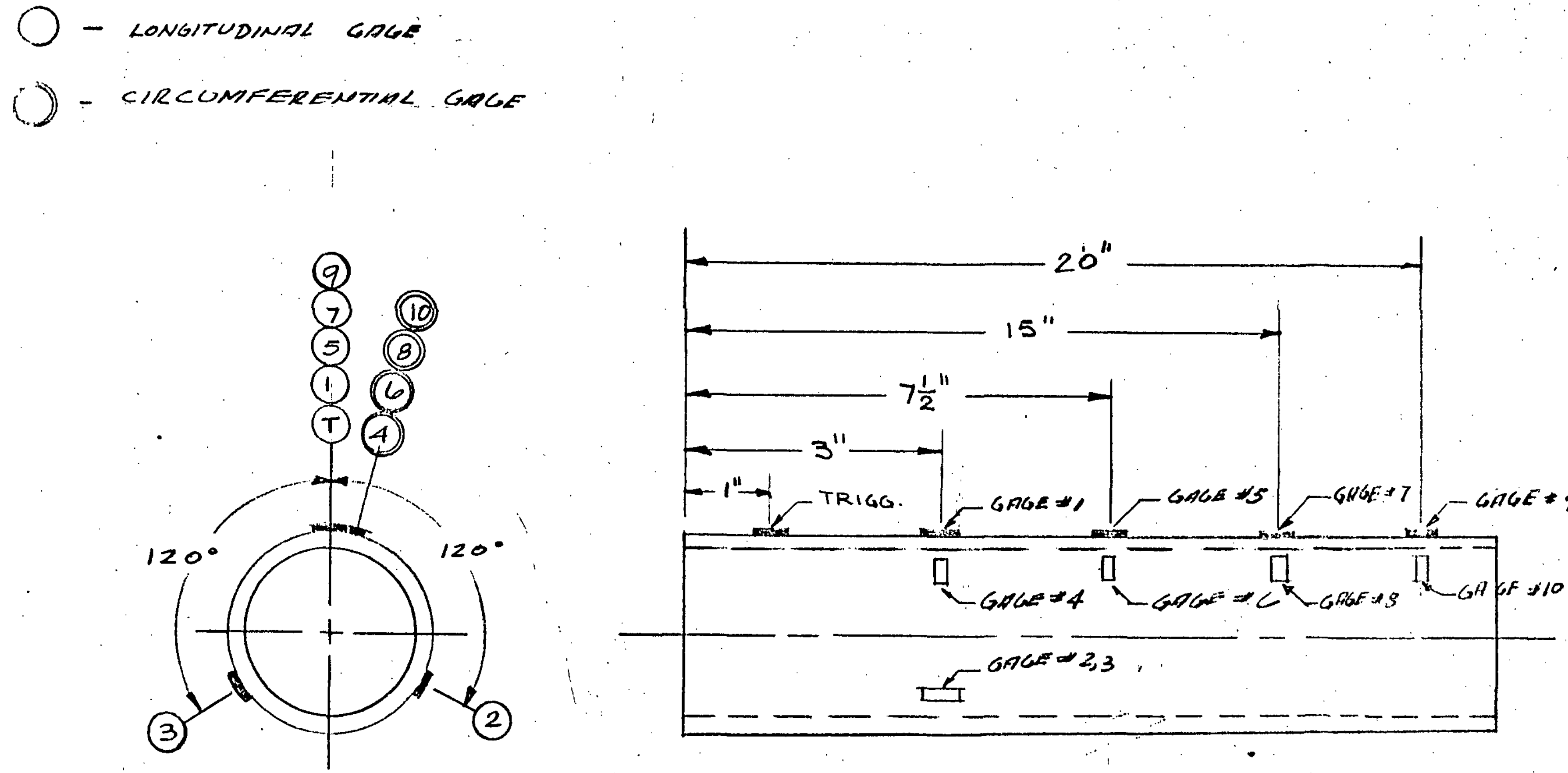

FIGURE 24

GAGE LOCATION FOR THE

SHEAR IMPACT EXPERIMENT

NOT TO SCALE

DRAWN : ARIE BLOM

DATE : NOV. 5. 1971

REV. : I JAN. 20. 1972

The repeatability of the results was difficult since there appeared to be slight deviations between the detonators. However, the resulting strain traces have the same characteristics and are very similar in shape.

A typical block diagram showing the circuitry, instruments, strain gages and the test specimens are shown in Fig. 25.

RESULTS

Typical oscilloscope traces are shown in Figs. 26 and 27. Observation of these figures show the presence of a bending wave propagating at the plate velocity, c_p, which is faster than the shear velocity, c_s. Figure 26 presents typical traces using the X-549 electrical detonator inserted in plexiglass. We obtained better results in this group of tests by using the circumferential gages no. 4 and 6 in Fig. 24. The measurement of the wave speeds yielded an average shear velocity of

$$c_s = 122{,}950 \text{ in/sec.}$$

The alignment gages show a reasonably good impact, but the presence of bending is shown by the difference in magnitude of the strain pulse between the alignment gages. However, a separation between the longitudinal and the shear wave are not clearly observed. Figure 27 presents typical traces using the X-811D electrical detonator embedded in lexan. Since the firing time is faster we used gages no. 7 and 9. The measurement of the wave speeds yielded

$$c_p = 214{,}500 \text{ in/sec.}$$

$$c_s = 125{,}000 \text{ in/sec.}$$

These values are slightly higher than the analytical values of

$$c_p = 205{,}333 \text{ in/sec.}$$

$$c_s = 113{,}338 \text{ in/sec.}$$

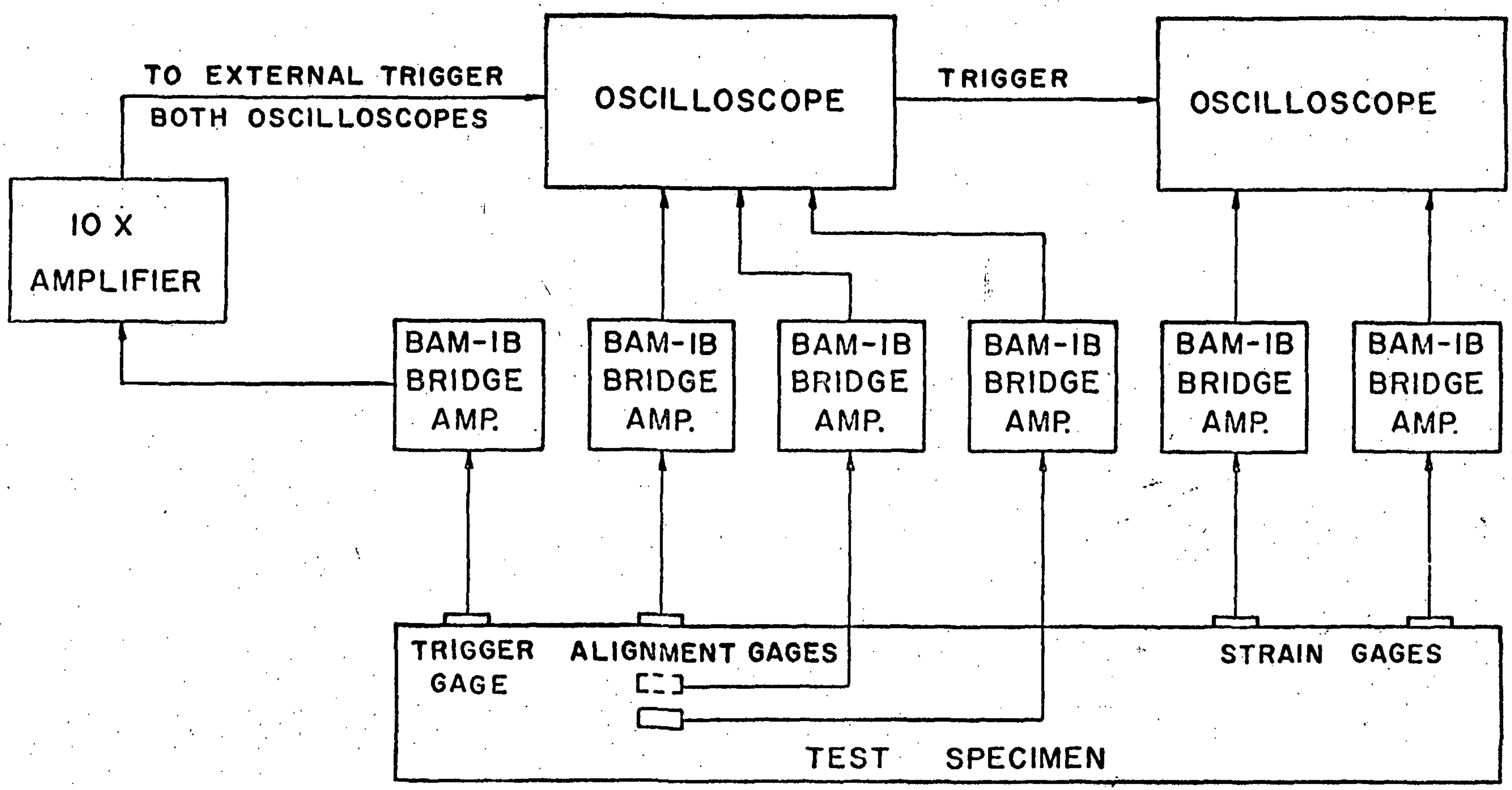

FIGURE 25 - TYPICAL BLOCK DIAGRAM OF CIRCUITRY, INSTRUMENTS AND TEST SPECIMEN

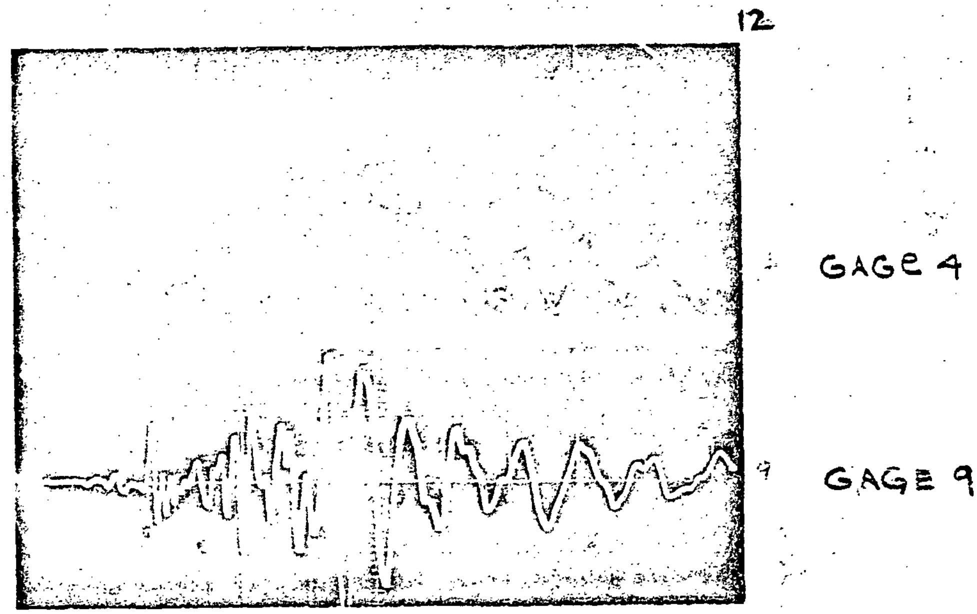

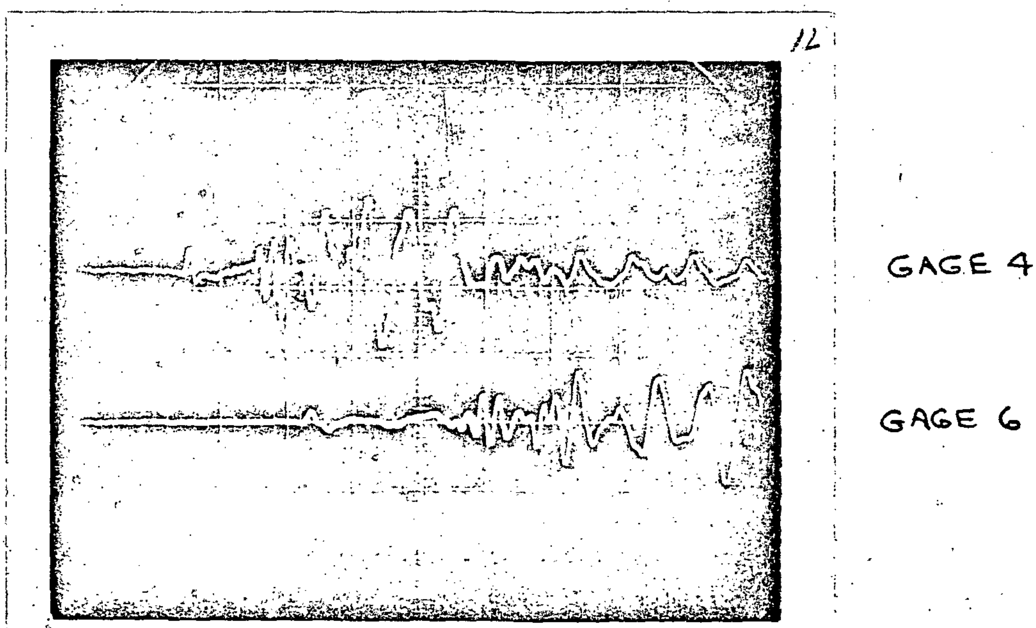

Horizontal Scale 20 μsec/DIV
Vertical Scale 500 μIN/IN/DIV

FIGURE 26 RESPONSE OF SHELL TO X-549 DETONATOR IN PLEXIGLASS PLUG

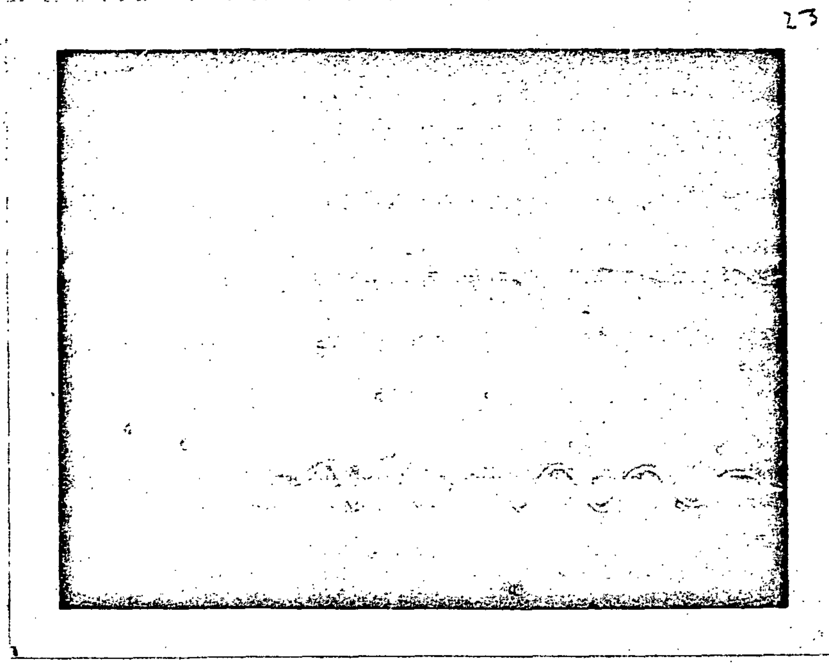

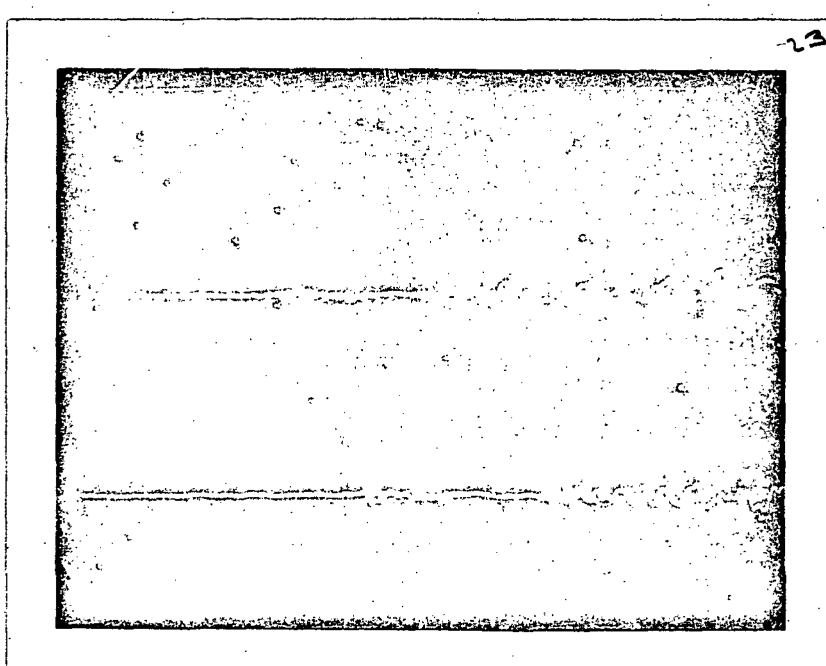

HORIZONTAL SCALE 20 μsec/DIV
VERTICAL SCALE 250 μIN/IN/DIV

FIGURE 27 RESPONSE OF SHELL TO X-11D DETONATOR IN LEXAN PLUG

Observation of Fig. 27 shows that the results obtained from the use of X-811D detonators are more consistent. The alignment gages show a better simultaneity of strain pulse than the previous types of electrical detonator.

A better comparison between theoretical and experimental shear wave speeds is probably impossible, since, the analytically predicted value involves the use of a shear correction factor. The exact specification of this factor is questionable.

CONCLUSION

In this section an experimental technique for generating and measuring shear wave velocities in cylindrical shells under radial impact is presented. Although the strain pulses are not simple in shape the arrival time of the pulse at a gage location is shown very clearly, from which the wave speed can be determined. There is still further investigation to be made in order to understand the transient response of a cylindrical shell to radial impact. However, the first step in this study was completed, namely the experimental verification of the speed of a shear wave propagating in cylindrical shell.

VII. CONCLUSIONS AND RECOMMENDATIONS

The conclusions of this study are briefly listed below.

1. For clean cylindrical shells subjected to longitudinal impact:

   a.) the single most important parameter effecting the magnitude of the shell's transient response is the ratio h/λ (λ being related to the pulse duration, τ_0, by $\lambda = \tau_0 c_p$). Except for the rectangular pulse, the peak values of strain or stress will always depend upon this ratio,

   b.) single-pulse dispersion (wave spreading) is dependent on h/λ in much the same manner as in the dispersion of continuous harmonic dispersion,

   c.) the shape of the pulse behind the wave front becomes indistinguishable for long pulse durations (small values of h/λ) and all the shapes studied here become similar as the pulse travels down the shell,

   d.) except for the uniaxial theory, which predicts constant shape and magnitude of propagating pulse, the membrane (with and without shear) and bending theories predict, for practical purposes, similar transient responses,

   e.) the use of a sine series to approximate the pulse shapes is a useful tool for predicting conceptual or actual transient responses. The response for each of the sine terms is computed and the result for a particular shape is obtained by superposition of these individual results.

2. For cylindrical shells having geometrical discontinuities subjected to longitudinal impact:

   a.) for short pulses having a short rise time (almost a step) the simple uniaxial result of

$$\frac{[\varepsilon_x]_{\text{transmitted}}}{[\varepsilon_x]_{\text{incident}}} = \frac{2A_1}{A_1+A_2},$$

can be used to predict the effect of the geometrical discontinuity on response.

b.) For longer pulse durations, the peak values occur behind the initial wave front and a computer calculation incorporating matching conditions at the geometrical discontinuity is required to predict the effect of the discontinuity on the transient response.

3. The generation of a shear wave in a cylindrical shell has been accomplished with the measured shear velocity agreeing, within 8%, with the analytically predicted value.

Recommendations for further work include.

1. Experimental verification of the variation of strain response with the h/λ ratio,
2. More analytical studies involving a larger range of geometrical discontinuities in the cylindrical shell,
3. Experimental verification of the results for the shell having a geometrical discontinuity,
4. An analytical study into the relationship between single pulse dispersion and the classical harmonic dispersion,
5. Further experimental work in the area of shear wave propagation and the transient response of shells to shear loadings,
6. An analytical study into the effect of the shape of a shear pulse on a shell's response,
7. A joint analytical - experimental study into the response of a structure to a combined longitudinal - shear excitation.

VIII. GENERAL

VIII. 1 - Relevance of Results

The results of the study presented in this Report can be applied directly to the following technical areas:

a. Response of Structures to Pyrotechnic Loads

Utilizing the results of this study into effects of pulse shapes or transient responses, we are in a position to predict the important parameters of the resulting loading pulse caused by a pyrotechnic event. In addition, we can apply the results of this study to the prediction of the effect of a structure's geometrical discontinuities on the resulting response of a structure subjected to a pyrotechnic event.

b. Understanding Ultrasonic Signals in Structures (NDT)

Since the thrust of this grant's study was the use of sine "building blocks", we have used the results of the transient response of the shell structure to these sine pulses in the interpretation of transmitted ultrasonic signals. The single most important result used for this purpose is the dispersive effect caused by the thickness to wavelength ratio (h/λ). For example, when transmitting an ultrasonic signal along a shell the magnitude (and shape) of this signal changes due to geometrical or material defects and dispersion. To date, in the field of NDT only limited information is available which will help in understanding which portion of the change in signal shape is due to defect and which portion is due to dispersion. The results of this year's grant are being applied to an ultrasonic study which will hopefully lead to a better understanding of this signal interpretation. The initial results are encouraging.

c. Response of Composite Material Structures to Dynamic Loads

Much of the information and technology developed in this year's grant (and previous years') is in the process of being applied to composite material structures, both homogeneous and laminated. The initial results show that these capabilities are directly applicable to problems, such as, FOD in engine or helicopter blades and the dynamic loading of composite structures by foreign objects, pyrotechnic events, or docking. For example, one of our initial results have shown that for certain laminate plate configurations subjected to dynamic moment inputs, large normal and shear stresses are developed in the laminate, which is not the case in isotropic plates. Realizing that laminates cannot withstand high shear stresses, this result is seen to be important for the proper design of laminate structures to withstand dynamic loads.

VIII. 2 - Personnel Involvement

3 - Faculty; Drs. R. Mortimer, P. Chou, and J. Rose

3 - Graduate Students; Messrs. Blum, Rodini, and Cokonis

2 - Undergraduate Students; Messrs. Flis and Nga Le

1 - Technician; Mr. R. Tschirschnitz

Of the three graduate students listed above, two are Ph.D. students and one is a Master's student. Mr. Blum has recently completed his Ph.D. thesis, which was supported by this grant.

IX. ADDITIONAL WORK COMPLETED UNDER GRANT

In addition to the studies described in Sections II through VIII, other work related to the thrust of this Grant, and supported by this Grant, was completed. A brief description of these tasks follows:

a. Equations Governing the Axisymmetric Motions of a Laminated Composite Cylindrical Shell.

A system of dynamic equations of motion which govern the motions of a laminated composite cylindrical shell have been derived. This system of equations was derived by combining the usual isotropic shell theory development (Ref. 1) with the technique developed for anisotropic laminated plates (Ref. 10). This theory includes the effects of transverse shear, rotary and radial inertia, and bending. The transverse shear effect is extremely important when considering laminated structures. The resulting system of equations can be used to analyze the dynamic (transient) axisymmetric response of a cylindrical shell which is constructed from a number of isotropic or anisotropic layers. The form of the resulting system of equations is

$$
\begin{aligned}
u'' &- \frac{\ddot{u}}{c_1^2} + (\quad)\, v'' = - - - - - \\
v'' &- \frac{\ddot{v}}{c_2^2} + (\quad)\, u'' = - - - - - \\
\psi_x'' &- \frac{\ddot{\psi}_x}{c_2^2} + (\quad)\, \psi_\theta'' = - - - - - \\
\psi_\theta'' &- \frac{\ddot{\psi}_\theta}{c_2^2} + (\quad)\, \psi_x'' = - - - - - \\
w'' &- \frac{\ddot{w}}{c_3^2} \qquad\qquad\quad = - - - - -
\end{aligned}
\qquad \text{(IX-1)}
$$

where u, v, w, ψ_x and ψ_θ denote the longitudinal, circumferential, and radial displacement, and the longitudinal and circumferential rotations, respectively; c_1, c_2, c_3 are wave speed parameters. The parenthesis appearing on the left-hand side of these equations involve material and geometric properties; the right-hand side of these equations involve the five displacements and their first derivatives. This theory can be extended to include conical shells.

b. Computer Code for the Dynamic Analysis of Laminated Structures.

A computer code, based on the method of characteristics, capable of solving systems of equations equivalent to eq. (IX-1) has been written. Example runs to test the accuracy of this program still remain to be completed. This code, in addition to existing codes at Drexel, enable us to analyze the transient behavior of composite laminate shells, plates, and beams where each individual lamina may be isotropic or anisotropic.

c. Cylindrical Shell with Finite Length Geometrical Discontinuity.

A computer code capable of analyzing the transient behavior of a shell having a finite length geometrical discontinuity has been developed. This code is an extension of the work reported in Ref. 5.

d. Shear Wave Computer Code.

A computer code capable of analyzing the transient response of structures to step loadings in transverse shear has been developed.

X. REFERENCES

1. Mortimer, R., Rose, J., and Chou, P., "Longitudinal Impact of Cylindrical Shells," Exp. Mechs., January 1972, pp. 25-31.
2. Mortimer, R., and Hoberg, J., "MCDIT-21 - A Computer Code for One-Dimensional Elastic Wave Problems," NASA CR-1306, April 1969.
3. Berkowitz, H., "Longitudinal Impact of a Semi-Infinite Elastic Cylindrical Shell," JAM, September 1963, pp. 347-354.
4. Rose, J. and Mortimer, R., "Applications of Elastic Wave Analysis in Nondestructive Testing," presented at Fall Meeting of ASNT, Detroit, Mich., October 1971. Also submitted for publication.
5. Mortimer, R., Rose, J., and Blum, A., "Longitudinal Impact of Cylindrical Shells with Discontinuous Cross-Sectional Area," ASME paper No. 72-APM-24, to appear in Journal of Applied Mechanics.
6. Mayer, G. W., "Determination of Ultrasonic Velocities by Measurement of Angles of Total Reflection," Journal of the Acoustical Soc. of America, Vol. 32, No. 10, October 1960, pp. 1213-1215.
7. King, M. S., and Falt, I., "Ultrasonic Shear-Wave Velocity in Rocks Subjected to Simulated Overburden Pressure," Geophysics, Vol. XXVII, No. 5, October 1962, pp. 590-598.
8. Von Steveninck, J., "Apparatus for Simultaneous Determination of Longitudinal and Shear Wave Velocities Under Pressure," Journal of Scientific Instruments, Vol. 44, No. 5, May 1967, pp. 379-381.
9. Bahjat, P., Kisszinger, C., "Model Study of Radiation from an Explosion in a Circular Disk," Geophysics, Vol. 34, No. 2, April 1969.
10. Whitney, J. and Pagano, N., "Shear Deformation in Heterogeneous Anisotropic Plates," Tech. Report AFML-TR-70-31, July 1970.

X. APPENDICIES

APPENDIX A

EQUATIONS GOVERNING THE MOTION OF A CYLINDRICAL SHELL

Four systems of governing differential equations were used in this study. These equations, as presented here, are nondimensionalized with respect to h such that

$$\bar{u} = \frac{u}{h}, \quad \bar{\psi} = \psi, \quad \bar{w} = \frac{w}{h}, \quad \bar{x} = \frac{x}{h}, \quad \bar{\tau} = \frac{t\, c_p}{h}$$

The first system of equations includes membrane, bending, transverse shear, and rotary inertia effects and is given by (see Ref. 1)

$$\frac{\partial^2 \bar{u}}{\partial \bar{x}^2} - \frac{\partial^2 \bar{u}}{\partial \bar{\tau}^2} = -\nu \frac{h}{R} \frac{\partial \bar{w}}{\partial \bar{x}}$$

$$\frac{\partial^2 \psi}{\partial \bar{x}^2} - \frac{\partial^2 \psi}{\partial \bar{\tau}^2} = \left(\frac{h}{R}\right)^2 \frac{g}{\eta(1-\eta)} \psi + \left(\frac{h}{R}\right)^2 \frac{(g + \eta\nu)}{\eta(1-\eta)} \frac{\partial \bar{w}}{\partial \bar{x}} \qquad \text{(A-1)}$$

$$\frac{\partial^2 \bar{w}}{\partial \bar{x}^2} - \left(\frac{c_p}{c_s}\right)^2 \frac{\partial^2 \bar{w}}{\partial \bar{\tau}^2} = \left(\frac{h}{R}\right) \frac{\nu}{g} \frac{\partial \bar{u}}{\partial \bar{x}} - \left(1 + \frac{\eta\nu}{g}\right) \frac{\partial \psi}{\partial \bar{x}} + \left(\frac{h}{R}\right)^2 \frac{(1+\eta)}{g} \bar{w}$$

The second system of equations represents a modified membrane theory and is given by (see Ref. 1)

$$\frac{\partial^2 \bar{u}}{\partial \bar{x}^2} - \frac{\partial^2 \bar{u}}{\partial \bar{\tau}^2} = -\nu \frac{h}{R} \frac{\partial \bar{w}}{\partial \bar{x}}$$

$$\qquad \text{(A-2)}$$

$$\frac{\partial^2 \bar{w}}{\partial \bar{x}^2} - \left(\frac{c_p}{c_s}\right)^2 \frac{\partial^2 \bar{w}}{\partial \bar{\tau}^2} = \left(\frac{h}{R}\right) \frac{\nu}{g} \frac{\partial \bar{u}}{\partial \bar{x}} + \left(\frac{h}{R}\right)^2 \frac{(1+\eta)}{g} \bar{w}$$

The third system of equations represents the classical membrane theory and is given by

$$\frac{\partial^2 \bar{u}}{\partial \bar{x}^2} - \frac{\partial^2 \bar{u}}{\partial \bar{\tau}^2} = - \nu \frac{h}{R} \frac{\partial \bar{w}}{\partial \bar{x}}$$

$$- \left(\frac{c_p}{c_s}\right)^2 \frac{\partial^2 \bar{w}}{\partial \bar{\tau}^2} = \left(\frac{h}{R}\right) \frac{\nu}{g} \frac{\partial \bar{u}}{\partial \bar{x}} + \left(\frac{h}{R}\right)^2 \frac{(1 + \eta)}{g} \bar{w} \tag{A-3}$$

The final system of equations is the simple uniaxial theory and is given by

$$\frac{\partial^2 \bar{u}}{\partial \bar{x}^2} - \frac{\partial^2 \bar{u}}{\partial \bar{\tau}^2} = 0 \tag{A-4}$$

APPENDIX B

LEAST SQUARES LINEAR ESTIMATION

Capabilities of Program

The program will:

1. Compute coefficients to any linear relation
2. Print and plot results on printout.

e.g.

$$F(x,y,z) \cong A_o + A_1 V_1(x,y,z) + A_2 V_2(x,y,z) \ldots A_n V_n$$

$F(x,y,z)$ – Function being estimated

$V_i(x,y,z)$ – Estimating functions

(x,y,z) – Independent coordinate variables

$A_o \rightarrow A_n$ – Coefficients computed by program

Note:

(A) Approximation takes place on a finite interval

(B) All functions must be bounded

(C) All functions must be defined on the same coordinate system - Coordinate system can be comprised of any number of independent variables. e.g.:

$$F(x), F(x, r, \theta), F(z, Y, V_1, V_2)$$

(D) All functions can be discontinuous.

```
/PROGRAM AJC,PAGES=40,TIME=20,LINES=65
C*************************************************************************
C
C     L E A S T   S Q U A R E S   L I N E A R   E S T I M A T I O N
C
C*************************************************************************
C
C         F(X,Y,Z)--- A0 + A1*V1(X,Y,Z) + A2*V2(X,Y,Z).......AN*VN
C
C
C         F(X,Y,Z) ----- ESTIMATED FUNCTION (PROGRAMER SPECIFIED)
C
C         V(I)(X,Y,Z) -- ESTIMATING FUNCTIONS (PROGRAMER SPECIFIED)
C
C         A(I) --------- COEFFICIENTS COMPUTED BY PROGRAM
C
C         (X,Y,Z) ------ INDEPENDANT COORDINATE VARIABLES
C
C
C         NOTE: (A) ESTIMATION TAKES PLACE ON A FINITE INTERVAL
C               (B) ALL FUNCTIONS MUST BE BOUNDED
C               (C) ALL FUNCTIONS MUST BE DEFINED ON THE SAME COORDINATE
C                   SYSTEM - COORDINATE SYSTEM CAN BE COMPRISED OF ANY
C                   NUMBER OF INDEPENDANT VARIABLES
C               (D) ALL FUNCTIONS CAN BE DISCONTINUOUS
C*************************************************************************
      DOUBLE PRECISION   BB,BS,AS,T,AA,ASS
      DOUBLE PRECISION DEXP,PI,DSIN,  RNH
      DOUBLE PRECISION RR,TY
      DOUBLE PRECISION DS
      DOUBLE PRECISION DABS
      DOUBLE PRECISION ASP,A,B,SAP,X,Y,TS1,TS2,S1,S2,RMS,RM,TYF,YF,TNO
      DIMENSION AA(20,20),C(1000)
       DIMENSION A(20,20)
      DIMENSION  B(90,20),BB(20,20)
      COMMON/AP/NO,NV,NDV,NDI,ND,IC
      COMMON ANG(9),BLANK,STAR
      COMMON/PP/VAR(20,10),VAD(20,10)
C*************************************************************************

         PROGRAM INPUT CONSTANTS
```

```
C*****************************************************************************
      ND=41
      NV=3
      NDV=4
      NDI=1
      ND=1
      IC=0
C*****************************************************************************
C
C        ND = NO. OF POINTS AT WHICH ALL FUNCTIONS ARE EVALUATED
C
C
C        NV = NO. OF ESTIMATING FUNCTIONS
C
C
C        NDV = NO. OF ESTIMATED FUNCTIONS
C
C
C        IC = 0 - A(0) (ZERO ORDER COEFFICIENT) IS NOT COMPUTED
C
C             1 - A(0) COMPUTED
C
C
C        NDI =  MINIMUM ORDER  POWER SERIES
C
C        ND. =  MAXIMUM ORDER  POWER SERIES
C
C             NOTE : THE PROGRAM WILL COMPUTE COEFFICIENTS FOR EACH POWER
C                    EXPANSION OF THE MEMBER FUNCTIONS. IT WILL START WITH
C                    ORDER NDI,THEN NDI+1,NDI+2 UP TO ND . IF FUNCTIONS ARE TO
C                    BE LEFT AS ORDER ONE THEN NDI=ND=1
C
C                   FOR EXAMPLE :  SPECIFYING NDI=1  ND=3
C
C                    THE PROGRAM WILL COMPUTE ALL COEFFICIENTS
C                    OF THE FOLLOWING SET OF EXPANSIONS:
C
C                    Y = A(0) + A(1)*X(1) + A(2)*X(2)
C
C                    Y = B(0) + B(1)*X(1) + B(2)*X(2) + B(3)*X(1)**2 +
C                        B(4)*X(2)**2
```

```
C
C                      Y = C(0) + C(1)*X(1) + C(2)*X(2) + C(3)*X(1)**2 +
C                          C(4)*X(2)**2 + C(5)*X(1)**3 + C(6)*X(2)**3
C
C*****************************************************************************
    5 FORMAT(11A1)
      READ (5, 5) BLANK,(ANG(I),I=1,9),STAR
  100 FORMAT (13X,20A1)
  101 FORMAT(15X,20A1)
      DO102L=1,NV
  102 READ 100,(VAR(I,L),I=1,20)
      DO103L=1,NDV
  103 READ 101,(VAD(I,L),I=1,20)
      NT=ND*NV
      NT1=NT+1
      NT2=NT+2
      NT3=NT+3
      NT4=NT+4
      NT5=NT+5
      NT6=NT+6
      NTL=NT+NDV
      NH=NO
      NH1=NO
      RNH=NO-1
      PI=3.14159265359
      DO 21K=1,NO
      DO 20 L=1,NT1
      B(K,L)=0.
      KS=K+L*NO
   20 C(KS)=0.
      Y=K-1
      X=Y/RNH
   21 C(K)=X
      DO 30L=1,NO
      K=L-1
      Y=K
      X=Y/RNH
C*****************************************************************************
C
C          ENTER ESTIMATING FUNCTIONS IN COLUMNS  1,2,3,...NV  OF MATRIX  B
C
C          FOR EXAMPLE:
```

```
      B(L,1)=DSIN(PI*X)
      B(L,2)=DSIN(PI*X*2.)
      B(L,3)=DSIN(PI*X*3.)
C*****************************************************************************
C
C
C
C*****************************************************************************
C
C         ENTER ESTIMATED FUNCTIONS IN COLUMNS NT1,NT2,NT3......NTL  OF MATRIX B
C
C         FOR EXAMPLE :
      IF(X-.905)95,95,96
   95 B(L,NT1)=1.
      GO TO 97
   96 B(L,NT1)=1.-(X-.905)/.095
   97 CONTINUE
      IF(L-NH/2)10,10,11
   10 B(L,NT2)=2.*X
      GO TO 6
   11 B(L,NT2)=-2.*X+2.
    6 CONTINUE
    8 B(L,NT3)=-X+1.
      B(L,NT4)=(DSIN(PI*X))**2
C*****************************************************************************
C
C
C
   30 CONTINUE
C*****************************************************************************
C
C         INPUT FOR APLOT
C
C                NOTE : REMOVE FOLLOWING STATEMENTS IF NV>9
C
C*****************************************************************************
      DO4K=1,NTL
      KK=K
      KK=KK*NO
      DO4L=1,NO
      LL=L+KK
    4 C(LL)=B(L,K)
```

```
C*********************************************************************
C
C         APLOT PLOTS ESTIMATING FUNCTIONS
C
C                NOTE : REMOVE FOLLOWING STATEMENTS IF NV>9
C
C*********************************************************************
      NV1=NV+1
      CALLAPLOT( 0,C,NO,NV1,0)
C*********************************************************************
C
C         COMPUTATION OF COEFFICIENTS AND PRINTING OF RESULTS
C
C*********************************************************************
      CALL FILMAT(B,BB)
      CALL SOLV (BB)
      DO500KK=NDI,ND
      MA=NV*KK   +IC
      M1A=MA-1
      MA1=MA+1
      CALL SORT(A,BB,MA)
      CALL DIAG(A,MA)
      CALL PRINTS(A,B,C,MA)
  500 CONTINUE
C*********************************************************************
C
C         ---- D A T A   I N P U T ----
C
C123456789*        NOTE: FIRST SPACE IS BLANK
C
C
C         A DUPLICATE OF EACH EXECUTION CARD CONTAINING FIRST ALL THE ESTIMATING
C         FUNCTIONS AND SECOND ALL ESTIMATED FUNCTIONS.FOR EXAMPLE :
C     B(L,1)=DSIN(PI*X)
C     B(L,2)=DSIN(PI*X*2.)
C     B(L,3)=DSIN(PI*X*3.)
C  95 B(L,NT1)=1.
C             2.*X  ,-2.*X+2
C   8 B(L,NT3)=-X+1.
C     B(L,NT4)=(DSIN(PI*X))**2
C
C*********************************************************************
```

```
C
C        ----SUBROUTINE DESCRIPTION ----
C
C        FILMAT - COMPUTES LINEAR EQUATONS MATRIX
C
C        SOLV  - UPPER DIAGONALIZES LINEAR COEFFICIENT MATRIX (GAUSIAN
C                ELIMINATION).
C
C        SORT - TRANSFERS A PORTION OF UPPER DIAG MATRIX THAT IS ASSOCIATED WITH
C                A PARTICULAR EXPANSION
C
C        DIAG - SOLVES FOR COEFFICIENTS BY BACK MULTIPLICATION OF DIAG MATRIX
C
C        PRINTS - PRINTS OUT TITLES AND PLOTS RESULTS
C
C        APLOT - PLOTING ROUTINE
C
C****************************************************************************
 2002 STOP
      END
```

```
      SUBROUTINE FILMAT(B,BB)
      DOUBLE PRECISION B,BB,AS
      DIMENSION  B(90,20),BB(20,20)
      COMMON/AP/ND,NV,NDV,NDI,NO,IC
      NT=ND*NV
      NT1=NT+1
      NTL=NT+NDV
      IF(ND-1)1,1,2
    2 CONTINUE
      DO314M=1,NO
      NP=NV
      DO315K=2,ND
      DO301L=1,NV
      NP=1+NP
      IF(B(M,L))312,313,312
  312 B(M,NP)=B(M,L)**K
      GO TO 301
  313 B(M,NP)=0.
  301 CONTINUE
  315 CONTINUE
  314 CONTINUE
    1 CONTINUE
      IF(IC)11,10,11
   11 CONTINUE
      BB(1,1)=NO
      DO304K=1,NTL
      KS=K+1
      AS=0.
      DO305M=1,NO
      AS=AS+B(M,K)
  305 CONTINUE
      BB(1,KS)=AS
      BB(KS,1)=AS
  304 CONTINUE
   10 CONTINUE
      DO302N=1,NT
      N1=N+IC
      DO302K=N,NTL
      KS=K+IC
      AS=0.
      DO303M=1,NO
      AS=B(M,K)*B(M,N)+AS
  303 CONTINUE
      IF(NT1-K)4,3,3
    3 CONTINUE
      BB(N1,KS)=AS
      BB(KS,N1)=AS
      GO TO 302
    4 CONTINUE
      BB(N1,KS)=AS
  302 CONTINUE
      RETURN
      END
```

```
      SUBROUTINE SOLV(A)
      DOUBLE PRECISION A,X,ASP,SAP
      DIMENSION A(20,20)
      COMMON/AP/NO,NV,NDV,NDI,ND,IC
      MA=NV*ND  +IC
      MA1=MA+1
      M1A=MA-1
      MAL=MA+NDV
      DO100L=1,M1A
      L1=L+1
      NS=-10
      DO101N=L,MA
      IF(A(N,L))102,101,102
  102 NS=N
      GO TO 103
  101 CONTINUE
  103 IF(NS-L)113,106,105
  105 DO104N=1,MAL
      X=A(L,N)
      A(L,N)=A(NS,N)
  104 A(NS,N)=X
  106 ASP=1./A(L,L)
      DO200N=L1,MAL
      A(L,N)=ASP*A(L,N)
  200 CONTINUE
      DO107N=L1,MA
      IF(A(N,L))108,107,108
  108 SAP=1./A(N,L)
      DO109K=L1,MAL
      A(N,K)=A(N,K)*SAP    -A(L,K)
  109 CONTINUE
  107 CONTINUE
  100 CONTINUE
      DO 1K=MA1,MAL
      A(MA,K   )=A(MA,K   )/A(MA,MA)
    1 CONTINUE
  113 CONTINUE
      RETURN
      END
```

```
      SUBROUTINE DIAG(A,MA)
      DOUBLE PRECISION A
      DIMENSION A(20,20)
      COMMON/AP/NO,NV,NDV,NDI,ND,IC
      MA1=MA+1
      M1A=MA-1
      MAL=MA+NDV
      DO11L=MA1,MAL
      DO110N=1,M1A
      N1=MA1-N
      N2=N1-1
  114 DO111K=1,N2
      A(K,L   )=A(K,L   )-A(K,N1)*A(N1,L   )
  111 CONTINUE
  110 CONTINUE
   11 CONTINUE
      RETURN
      END
```

```
      SUBROUTINE PRINTS(A,B,C,MA)
      DOUBLE PRECISION A,B,RM,TY,RR
      DIMENSION A(20,20),B(40,20),C(1000)
      COMMON/AP/NO,NV,NDV,NDI,ND,IC
      COMMON/PP/VAR(20,10),VAD(20,10)
      COMMON ANG(9),BLANK,STAR
  100 FORMAT(1H1,//,20X,' E S T I M A T E D   F U N C T I O N : Y =',20A
     11,//)
   44 FORMAT(///,15X,'ESTIMATED',10X,'COMBINED FUNCTIONS',9X,'DIFFERANC'
     1,14X,'   X    ')
   45 FORMAT(//,20X,' LINEARLY COMBINED ESTIMATING FUNCTIONS',/ )
   43 FORMAT(4(10X,F14.7))
   40 FORMAT(20X,'(',D14.7,')*(',20A1,')**(',I2,')')
   41 FORMAT(/'  RMS DIFF = ',D14.7,/)
   42 FORMAT(' ',D14.7,' = CONSTANT')
   46 FORMAT (//,' COMPARISON BETWEEN ESTIMATED FUNCTION AND LINEARLY CO
     1MBINED ESTIMATING FUNCTIONS')
      KS=1-IC
      MA1=MA+1
      M1A=MA-1
      MAL=MA+NDV
      NT=NV*ND
      NT1=NT+1
      KK=(MA-IC)/NV
      DO50L=MA1,MAL
      LL=NT1+L-MA1
      K=L-MA
      PRINT 100,(VAD(I,K),I=1,20)
      PRINT 45
      IF(IC-1)4,2,4
    2 PRINT42,A(1,L)
    4 CONTINUE
      I=IC
      DO1IO=1,KK
      DO1IV=1,NV
      I=I+1
    1 PRINT 40,A(I,L),(VAR(J,IV),J=1,20),IO
      PRINT 46
      PRINT 44
      RM=0.
      DO310N=1,NO
      IF(KS-1)11,10,11
   10 CONTINUE
      TY=A(1,L    )*B(N,KS)
      GO TO 12
   11 CONTINUE
      TY=A(1,L    )
   12 CONTINUE
      DO311K=1,M1A
      K1=K+1
      K2=K+KS
      TY=B(N,K2)*A(K1,L    )+TY
  311 CONTINUE
      RR=TY-B(N,LL )
      L2=NO+N
      L3=NO+L2
      L4=NO+L3
```

PRINTS (CONT)

```
      C(L 2)=B(M,LL )
      C(L 3)=TY
      C(L 4)=RR
      PRINT 43,B(M,LL ),TY,RR,C(N)
      RM=RR*RR+RM
  310 CONTINUE
      RM=RM**.5/FLOAT(NC)
      WRITE(6,41)RM
      K=L-MA
      CALL APLOT(K,C,NO,4,0)
   50 CONTINUE
      RETURN
      END
```

```
      SUBROUTINE SORT(A,BB,MA)
      DOUBLE PRECISION A,BB,BS
      DIMENSION A(20,20),BB(20,20)
      COMMON/AP/NO,NV,NDV,NDI,ND,IC
      MA1=MA+1
      M1A=MA-1
      MAL=MA+NDV
      NT=ND*NV+IC
      NT1=NT+1
      DO307I=1,M1A
      I1=I+1
      A(I,I)=BB(I,I)
      DO307J=I1,MA
      BS=BB(I,J)
      A(I,J)=BS
      A(J,I)=BS
  307 CONTINUE
      A(MA,MA)=BB(MA,MA)
      DO1I=1,MA
      DO1L=MA1,MAL
      LL=NT1+L-MA1
    1 A(I,L)=BB(I,LL)
      RETURN
      END
```

```
C
C        ...............................................................
C
C        SUBROUTINE APLOT
C
C        PURPOSE
C           PLOT SEVERAL CROSS-VARIABLES VERSUS A BASE VARIABLE
C           DIRECT PLOTING OF INPUT VARIABLES (NO INTERPOLATION)
C
C        USAGE
C           CALL APLOT(NO,A,N,M,NS)
C
C        DESCRIPTION OF PARAMETERS
C           NO - CHART NUMBER (3 DIGITS MAXIMUM)
C           A  - MATRIX OF DATA TO BE PLOTTED. FIRST COLUMN REPRESENTS
C                BASE VARIABLE AND SUCCESSIVE COLUMNS ARE THE CROSS-
C                VARIABLES (MAXIMUM IS 9).
C           N  - NUMBER OF ROWS IN MATRIX A
C           M  - NUMBER OF COLUMNS IN MATRIX A (EQUAL TO THE TOTAL
C                NUMBER OF VARIABLES). MAXIMUM IS 10.
C           NS - CODE FOR SORTING THE BASE VARIABLE DATA IN ASCENDING
C                ORDER
C                  0  SORTING IS NOT NECESSARY (ALREADY IN ASCENDING
C                     ORDER).
C                  1  SORTING IS NECESSARY.
C
C        REMARKS
C  THE FOLLOWING EXECUTION CARDS NEEDED IN MAIN PROGRAM
C     COMMON ANG(9),BLANK,STAR
C     READ (5, 5) BLANK,(ANG(I),I=1,9),STAR
C   5 FORMAT(11A1)
C  THE FOLLOWING DATA CARD NEEDED IN MAIN PROGRAM
C  STARTING IN COULUMN #1
C                             .123456789*
C                             .   IS A BLANK SPACE
C
C        SUBROUTINES AND FUNCTION SUBPROGRAMS REQUIRED
C           NONE
C
C        ...............................................................
C

      SUBROUTINEAPLOT(NO,A,N,M,    NS)
      DIMENSION OUT(116),YPR(11)        ,A(1000)
      COMMON ANG(9),BLANK,STAR
C
    1 FORMAT(1H1,60X,7H CHART ,I3,//)
    2 FORMAT(1H ,F11.4,5X,101A1)
    3 FORMAT(/,20X,'>>>>>>>>>> E S T I M A T I N G   F U N C T I O N S
     1 <<<<<<<<<<',//)
    7 FORMAT(1H ,16X,101H.         .         .         .         .
     1    .         .         .         .         .         .)
    8 FORMAT(1H0,9X,11F10.4)
C
C        ...............................................................
C
      NLL=1
```

APLOT (CONT)

```
C
      IF(NS) 16, 16, 10
C
C         SORT BASE VARIABLE DATA IN ASCENDING ORDER
C
   10 DO 15 I=1,N
      DO 14 J=I,N
      IF(A(I)-A(J)) 14, 14, 11
   11 L=I-N
      LL=J-N
      DO 12 K=1,M
      L=L+N
      LL=LL+N
      F=A(L)
      A(L)=A(LL)
   12 A(LL)=F
   14 CONTINUE
   15 CONTINUE
C
C         TEST NLL
C
   16 IF(NLL) 20, 18, 20
   18 NLL=50
C
C         PRINT TITLE
C
   20 WRITE(6,1)NO
      IF(NO.EQ.0)PRINT3
C
C         FIND SCALE FOR CROSS-VARIABLES
C
      M1=N+1
      YMIN=A(M1)
      YMAX=YMIN
      M2=M*N
      DO 40  J=M1,M2
      IF(A(J)-YMIN) 28,26,26
   26 IF(A(J)-YMAX) 40,40,30
   28 YMIN=A(J)
      GO TO 40
   30 YMAX=A(J)
   40 CONTINUE
      YSCAL=(YMAX-YMIN)/100.0
C
C         FIND BASE VARIABLE PRINT POSITION
C
      MY=M-1
      DO 701L=1,N
```

APLOT (CONT)

```
C
C          FIND CROSS-VARIABLES
C
   50 DO 55 IX=1,116
   55 OUT(IX)=BLANK
      DO100IC=1,111,10
  100 OUT(IC)=STAR
      DO 60 J=1,NY
      LL=L+J*N
      JP=((A(LL)-YMIN)/YSCAL)+1.0
      OUT(JP)=ANG(J)
   60 CONTINUE
C
C          PRINT LINE AND CLEAR, OR SKIP
C
      XPR=A(L)
      WRITE(6,2)XPR,(OUT(IZ),IZ=1,101)
  701 CONTINUE
C
C          PRINT CROSS-VARIABLES NUMBERS
C
   86 WRITE(6,7)
      YPR(1)=YMIN
      DO 90 KN=1,9
   90 YPR(KN+1)=YPR(KN)+YSCAL*10.0
      YPR(11)=YMAX
      WRITE(6,8)(YPR(IP),IP=1,11)
      RETURN
      END
```